

University of Belgrade  
Faculty of Technology and Metallurgy

Almabrok A. Ashor

**Influence of interphase bonding of acrylate matrix with alumina reinforcement on mechanical and adhesion properties of composite**

Doctoral dissertation

Belgrade, 2020

Univerzitet u Beogradu  
Tehnološko-metalurški fakultet

Almabrok A. Ashor

**Uticaj načina ostvarivanja veze između  
ojačanja i matrice u kompozitu na bazi  
akrilata i čestica aluminijum-oksida na  
adhezionu i mehanička svojstva kompozita**

Doktorska disertacija

Beograd, 2020

Mentors

Dr Radmila Jančić Heinemann, full professor, University of Belgrade, Faculty of Technology and Metallurgy

Dr Marija Vuksanović, Senior Research Associate, University of Belgrade, “Vinča” Institute of Nuclear Sciences

.....  
Prof. dr Vesna Radojević, full professor,  
University of Belgrade, Faculty of  
Technology and Metallurgy

.....  
Prof. dr Aleksandar Marinković, Associate  
professor, University of Belgrade, Faculty  
of Technology and Metallurgy

.....  
Dr Nataša Tomić, Research Associate,  
Innovation Center, Faculty of Technology  
and Metallurgy

.....  
Dr Srdjan Tadić, Research Associate,  
Innovation Center, Faculty of Mechanical  
Engineering, University of Belgrade,

Candidate: \_\_\_\_\_

Date: \_\_\_\_\_

## ACKNOWLEDGEMENT

### *In the name of Allah, Most Gracious, Most Merciful*

I thank Allah (subhanahu wa ta'ala) for bestowing me with health, knowledge and patience to complete this work. Thereafter I would like to express my deep and sincere gratitude to my supervisors, Prof. Dr Radmila Jančić Heinemann and Dr Marija Vuksanović for giving me the opportunity to do this research and providing invaluable guidance throughout this research, without their guidance and persistent help this thesis has not been possible. It was a great privilege and honor to work and study under their guidance. Also, I would like to express my great appreciation to the thesis discussion committee Prof. Dr Vesna Radojević, Prof. Dr Aleksandar Marinković, Dr Nataša Tomić and Dr Srdjan Tadić.

Also, I would like to deeply thank my wife my sons and my daughters for their love, understanding, prayers and continuing support to complete this research work. Also, I express my thanks to my brothers and sisters for their devoted love, encouragement, and support.

Finally, my thanks go to all the people who have supported me to complete the research work directly or indirectly.

## **Summary**

### **Influence of interphase bonding in acrylate matrix with alumina reinforcement on mechanical and adhesion properties of composite**

Production engineering is a combination of manufacturing technology, engineering sciences. A production engineer typically has a wide knowledge of engineering practices and is aware of challenges related to production. In addition to this the materials science combines the properties, production methods and structure of materials and creates the matrix of knowledge that enables the successful design of a material. This thesis was oriented to synthesis and characterisation of a polymer matrix composite using specific ceramic particles.

The alumina particles are the one of the hardest materials when they have the corundum structure. On the other hand, alumina has also some fewer stable forms that have other uses and are a good material for designing the reinforcement of the composite. The aim of this thesis was to study the possibility of modification of the alumina particles surface using the silane modification and test the possibility of using the biodiesel, or the linseed oil ester as a surface modification of particles. The second of those modifications was only possible as a secondary layer on previously deposited silane. Those modifications had the main effect in preventing agglomeration of particles. The linseed oil ester added on the surface of the particles improved the hydrophobicity of particles and stabilizes the link of the modification later of silane to the surface of the particle. This is an important step to improve the behaviour of composites exposed to humidity and water.

Those particles were further used to produce composite films consisting of light polymerizing acrylates and those films were deposited on the brass substrate. This material exhibits good adhesion to the substrate and has improved hardness. The material itself has better characteristics compared to the polymer matrix alone. The improvement in adhesion performance can be attributed to the modified surface of particles and to the possible links that can be established not only between the reinforcement and the matrix but also between the composite and the substrate.

Creation of bulk composites having good mechanical properties and good surface resistance to cavitation was the aim of the part of research in this thesis. The material had improved biocompatibility as it was previously shown that the addition of itaconate into the poly (methyl methacrylate) improves the quantity of residual monomer. The aim was to create material having better characteristics in terms of hardness and cavitation resistance and it was shown that such composite having the alumina particles modified using the amiosilane, and biodiesel on the surface improves hardness of the material and with improving the hardness it improves the cavitation resistance. The cavitation resistance was tested using the standard mass loss procedure and it was compared to the morphology of surface specimens obtained after 60 min of exposure to cavitation. Image analysis gave the insight about the internal composition of the specimen and the resulting surface damage on the specimen. Finally, the toughness of specimens was tested using the control energy impact test and it was observed that the synthesized materials did not improve the toughness of the material. Only one of the observed specimens was better than the matrix itself.

Keywords: Polymer-matrix composites (PMCs)c, mechanical properties, adhesion, microstructures, cavitation erosion, impact testing

Scientific field: technological engineering

Narrow scientific field: materials engineering

## Sažetak

### **Uticaj načina ostvarivanja veze između ojačanja i matrice u kompozitu na bazi akrilata i čestica aluminijum-oksida na adhezioni i mehanička svojstva kompozita**

Proizvodno mašinstvo je kombinacija proizvodne tehnologije i inženjerskih nauka. Proizvodni inženjer obično ima široko znanje o inženjerskim praksama i svestan je izazova vezanih za proizvodnju. Pored ovoga, nauka o materijalima kombinuje svojstva, načine pripreme i strukturu materijala i stvara matricu znanja koja omogućava uspešno oblikovanje materijala. Ova doktorska disertacija bila je orijentisana na sintezu i karakterizaciju polimerno matričnog kompozita korišćenjem specifičnih keramičkih čestica.

Aluminijum oksidne čestice su jedne od najtvrdih materijala kada imaju strukturu korunda. Sa druge strane, aluminijum oksid ima i manje stabilne oblike koji imaju i drugu upotrebu i dobar su materijal za oblikovanje ojačanja kompozitnog materijala. Cilj ove teze bio je da se ispita mogućnost modifikacije površine čestica na bazi aluminijum oksida korišćenjem modifikacije silanom i ispita mogućnost upotrebe biodizela ili estra lanenog ulja kao površinske modifikacije čestica. Druga od ovih modifikacija bila je moguća samo kao sekundarni sloj na prethodno nataloženom silanu. Te modifikacije su imale glavni efekat u sprečavanju aglomerizacije čestica. Ester lanenog ulja, dodat na površinu čestica, poboljšava hidrofobnost čestica i stabilizuje vezu kasnije modifikacije silana sa površinom čestice. Ovo je važan korak u poboljšavanju ponašanja kompozitnog materijala izloženog kavitaciji.

Te čestice su dalje korišćene za proizvodnju kompozitnih filmova koji se sastoje od UV polimerizujućeg akrilata i ti su slojevi nanešeni na mesinganu podlogu. Ovaj materijal pokazuje dobru adheziju na podlozi i poboljšanu tvrdoću. Sam kompozitni materijal ima bolje karakteristike u poređenju sa samom polimernom matricom. Poboljšanje svojstava adhezije može se pripisati modifikovanoj površini čestica i mogućim vezama koje se mogu uspostaviti ne samo između ojačanja i matrice, već i između kompozitnog filma i supstrata.

Cilj rada ovoj tezi bio je stvaranje kompozitnih materijala koji imaju dobra mehanička svojstva i dobru površinsku otpornost na kavitaciju. Materijal je imao poboljšanu biokompatibilnost jer je prethodno pokazano da dodavanje itakonata u poli (metilmekralat) smanjuje količinu zaostalog monomera. Cilj je bio napraviti materijal sa boljim karakteristikama u pogledu tvrdoće i otpornosti na kavitaciju, a pokazano je da je takav materijal kompozit koji ima čestice aluminijum oksida modifikovane amiosilanom i biodizel na površini čestica. Otpornost na kavitaciju testirana je standardnim postupkom praćenjem gubitka mase i upoređena je sa morfologijom površinskih oštećenja dobijenih posle 60 minuta izloženosti kavitaciji. Analiza slike dala je uvid o unutrašnjem sastavu uzorka i rezultujućim površinskim oštećenjima na uzorku. Konačno, žilavost uzork testirana je korišćenjem testa kontrolisane energije i primećeno je da sintetisani materijali ne poboljšavaju žilavost materijala. Samo je jedan od posmatranih uzoraka bio bolji od same matrice.

Ključne reči: Polimer-matrični kompoziti, mehanička svojstva, adhezija, mikrostruktura, otpornost na kavitaciju, ispitivanje na udar

Naučna oblast: tehnološko inženjerstvo

Uža naučna oblast: inženjerstvo materijala



## List of publications

1. **“Almabrok A. Ashor, Marija M. Vuksanović, Nataša Z. Tomić, Aleksandar Marinković & Radmila Jančić Heinemann, 'The Influence of Alumina Particle Modification on the Adhesion of the Polyacrylate Matrix Composite Films and the Metal Substrate', Composite Interfaces, 26.5 (2019), 417-30.  
<https://doi.org/10.1080/09276440.2018.1506240>”**
2. **”Almabrok A. Ashor · Marija M. Vuksanović · Nataša Z. Tomić · Miloš Petrović · Marina Dojčinović · Tatjana Volkov Husović · Vesna Radojević · Radmila Jančić Heinemann. 2019. “Optimization of Modifier Deposition on the Alumina Surface to Enhance Mechanical Properties and Cavitation Resistance.” Polymer Bulletin 1–18. <https://doi.org/10.1007/s00289-019-02923-8>”**

## Contents

LIST OF TABLES .....	9
LIST OF FIGURES.....	10
INTRODUCTION.....	1
THEORETICAL PART	
1. COMPOSITES MATERIALS .....	3
1.1 CLASSIFICATION OF COMPOSITE MATERIALS .....	4
1.2 CONSTITUENTS OF COMPOSITE MATERIALS.....	4
1.3 CLASSIFICATION BASED ON MATRIX .....	5
1.3.1 Polymer Matrix Composites (PMC).....	5
1.3.2 Metal Matrix Materials.....	8
1.3.3 Ceramic Matrix Materials (CMM):.....	9
1.3.4 Carbon Matrices .....	10
1.4 CLASSIFICATION BASED ON REINFORCEMENT .....	10
1.4.1 Particle-Reinforced Composites .....	11
1.4.2 Fiber reinforcement .....	14
1.4.3 Laminar Composites.....	16
2. POLYMETHYL METHACRYLATE PMMA .....	17
2.1 Applications of Polymethyl methacrylate PMMA.....	18
2.2 Production Methods of Poly (methyl methacrylate) (PMMA).....	18
2.2.1 Radiation Initiated Polymerization of MMA.....	19
2.2.2 Heat Initiated Polymerization of MMA.....	19
2.2.3 Bulk Free Radical Polymerization and the Trommsdorf Effect .....	20
2.2.4 Solution Free Radical Polymerization.....	20
2.2.5 Suspension Polymerization .....	21
2.2.6 Emulsion Polymerization .....	22
2.3 Itaconates.....	22
2.4 Alumina $AL_2O_3$ .....	24
3. MATERIALS CHARACTERIZATION METHODS.....	26
EXPERIMENTAL PART	
4. SYNTHESIS OF ALUMINA PARTICLES AND THEIR SURFACE MODIFICATION.....	30
4.1 Preparation of alumina particles .....	31

4.2 Synthesis of methyl ester of linseed oil fatty acid (biodiesel – BD) .....	32
4.3 The first step of surface modification of alumina-based particles using 3-aminopropyl)tri – methoxy silane .....	34
4.4 The second step of alumina modification with BD .....	35
4.5. Results of particle surface modification discussion .....	36
4.5.1. XRD characterisation of particles.....	36
4.5.2. SEM characterisation of particles.....	36
4.5.3. Characterisation of the hydrophobisity of the particle surface modification.....	37
4.5.4. FTIR characterisation of particles surface modification .....	40
4.5.4. TG of surface-modified alumina-based particles .....	41
5. Composite films using modified and as produced alumina particles as reinforcement and photopolymerized matrix film.....	42
5.1 Composite films preparation .....	42
5.2 Hardness measurements of composite films – results and discussion.....	43
5.3 Hardness measurements for adhesion accesement – results and discussion.....	44
6 Composite materials having alumina particles, modified alumina particles and PMMA-itaconate matrix .....	49
6.1 Preparation of PMMA/DMI composites reinforced with alumina particles .....	49
6.2 Microhardness of composite materials – results and discussion .....	50
6.3 Testing of cavitation erosion - results and discussion .....	51
6.4 Image analysis used to characterize the surface degradation under cavitation of composite .....	53
6.5. AFM analysis of the composite specimen surface after surface erroision .....	60
6.6 Toughness of specimens measured by controlled energy impact testing .....	63
7. CONCLUSION .....	66
8. REFERENCES.....	69

## **LIST OF TABLES**

Table 1 the different types of thermosets and thermoplastic resins.....	8
Table 2 TGA analysis of alumina particles before and after surface modifications.....	42
Table 3 Hausforff dimension analysis of initial structures of composites having AM and BD modifications illustrating that the initial structure was mostly influenced by the way of preparation and that the resulting characterisation gave similar quantitative measurement .....	56
Table 4 “Comparison of hardness and surface damage parameters of samples exposed to cavitation after 60 minutes (samples with 5 wt. % of different alumina particles and two surface modifications)” .....	59

## LIST OF FIGURES

Figure 1. Composition of Composites .....	4
Figure 2. classifications of matrices.....	5
Figure 3. Kinds of thermosets.....	6
Figure 4. Kinds of thermoplastics.....	8
Figure 5. Schematic representation of composite materials classification .....	11
Figure 6. “Modulus of elasticity versus volume percent tungsten for a composite of tungsten particles dispersed within a copper matrix” .....	13
Figure 7. Structural formula of Polymethyl methacrylate PMMA .....	18
Figure 8. Structural formula of itaconic acid .....	23
Figure 9 Methyl ester of linseed oil fatty acid (biodiesel – BD) .....	32
Figure 10 Stoichiometry of reactions for methyl esters from triglycerides .....	33
Figure 11 Apparatus for vacuum distillation under nitrogen .....	34
Figure 12 The structure of 3-aminopropyl)tri – methoxy silane used as the primary modification of the surface of the alumina particles .....	35
Figure 13 a) Distribution of the diameter of synthesized ferrous oxide doped alumina particles and b) XRD of the synthesized ferrous oxide doped alumina particles after heat treatment at 900 °C .....	36
Figure 14. FE-SEM images of the particles: a) ferrous oxide doped alumina-based particles – Al <sub>2</sub> O <sub>3</sub> Fe, b) Al <sub>2</sub> O <sub>3</sub> Fe - AM particles and c) Al <sub>2</sub> O <sub>3</sub> Fe - BD particles .....	37
Figure 15. Schematic representation of surface hydrophobization and proposed interactions in a hydrophilic medium (H <sub>2</sub> O) .....	38
Figure 16. Wetting angle determination with a water droplet on a substrate obtained from: a) Al <sub>2</sub> O <sub>3</sub> Fe, b) Al <sub>2</sub> O <sub>3</sub> Fe-AM, and c) Al <sub>2</sub> O <sub>3</sub> Fe-BD particles .....	39
Figure 17. Comparison of FTIR spectra of ferrous oxide doped alumina-based particles used in composites preparation and after the hydrolysis .....	40
Figure 18. Micrograph of micro Vickers indentation for composite films: a) with 0.5 wt. % of Al <sub>2</sub> O <sub>3</sub> Fe - AM particles, and b) with 0.5 wt. % of Al <sub>2</sub> O <sub>3</sub> Fe - BD particles .....	43

Figure 19. a) Micro hardness changes regarding the amount of different modifications (AM/BD) of Al <sub>2</sub> O <sub>3</sub> Fe particles, b) the dependence of the adhesion strength parameter b of the particles share .	45
Figure 20. Dependence of the wetting angle for composite films in the moment of application on the substrate and after UV light exposure .	47
Figure 21. (I) Cross-section of the adhered composite films with (a) Al <sub>2</sub> O <sub>3</sub> Fe–AM particles, and (b) Al <sub>2</sub> O <sub>3</sub> Fe–BD particles, (II) contact surface of the (c) composite film and (d) substrate – brass .	48
Figure 22. a) The specimens for tensile testing b) The mold for sample preparation showing the forms for preparation of the sample for tensile testing and for high speed impact testing.	49
Figure 23. “Micro Vickers hardness of PMMA/DMI matrix and composites reinforced with a) ferrous oxide doped alumina-based particles and b) alumina nanoparticles” .	50
Figure 24. The experimental setup of the cavitation testing in the stationary fluid	51
Figure 25. “Mass loss during cavitation resistance testing of composites with different alumina-based particles: a) PMMA/DMI/Al <sub>2</sub> O <sub>3</sub> Fe AM, b) PMMA/DMI/ Al <sub>2</sub> O <sub>3</sub> Fe BD, c) PMMA/DMI/Al <sub>2</sub> O <sub>3</sub> n AM and d) PMMA/DMI/Al <sub>2</sub> O <sub>3</sub> n BD”	52
Figure 26. “Optical micrographs of surfaces of specimens prior to cavitation exposure having 5 wt. % of particles reinforced using the a) Al <sub>2</sub> O <sub>3</sub> Fe AM, b) Al <sub>2</sub> O <sub>3</sub> Fe BD, c) Al <sub>2</sub> O <sub>3</sub> n AM and d) Al <sub>2</sub> O <sub>3</sub> n BD” .	54
Figure 27. “The region on the surface of the specimen having 5 wt. % of alumina modified using AM reinforcement showing the obvious difference between the region subjected to cavitation and the region that was out of the reach of the jet”	55
Figure 28. “FE-SEM micrographs of surface morphology of composites after cavitation in PMMA/DMI matrix with 5 wt. % of: a) Al <sub>2</sub> O <sub>3</sub> Fe AM, b) Al <sub>2</sub> O <sub>3</sub> Fe BD, c) Al <sub>2</sub> O <sub>3</sub> n AM and d) Al <sub>2</sub> O <sub>3</sub> n BD”	57
Figure 29. “ a) Extraction of defects by adaptive trash hold defects selection and b) binary image mask used for surface defect characterization”	58
Figure 30. “SEM Section Analysis of composite with Al <sub>2</sub> O <sub>3</sub> Fe AM, (21µm x 16 µm): a) View of the analyzed surface, b) surface plot of the observed surface, c) line profile analysis”	61

Figure 31. AFM Section Analysis of composite with Al <sub>2</sub> O <sub>3</sub> Fe AM, (5μm x 5 μm x 1 μm): a) View of the analyzed surface, b) surface plot of the observed surface, c) line profile analysis .....	62
Figure 32. “Specimen for high-speed impact testing in the testing machine after impact” . .....	64
Figure 33. “Energy–time curves obtained from impact tests of samples with alumina- based reinforcement: a) PMMA/DMI/Al <sub>2</sub> O <sub>3</sub> Fe AM, b) PMMA/DMI/Al <sub>2</sub> O <sub>3</sub> Fe BD, c) PMMA/DMI/Al <sub>2</sub> O <sub>3</sub> n AM and d) PMMA/DMI/Al <sub>2</sub> O <sub>3</sub> n BD” .....	65

# **Theoretical part**



## **INTRODUCTION**

“Production engineers and Materials Science engineers study the relationship between materials' structure, performance, properties and synthesis, and producing new materials and new applications that meet the needs of society” [1]. Very often the processes for industrialization of the designed materials are carried out in cooperation of production engineers and materials engineers.

The field of composite materials is one of the central points in the second part of the 20<sup>th</sup> century and the use of man-made composite materials reached a lot of humans activates. New plains contain a lot of composite materials parts, some of the medical interventions are possible only because biocompatible composite materials are developed and new composites are becoming part of the everyday use in our time. On the other hand, natural composites are part of human civilization from the very beginning of the development and they sometimes serve as the inspiration to create new improved materials.

Composite is a material that combines at least two materials that are separated by the interphase. This interphase not only separates the materials but has a vital role in composite material performance. The role of this interphase can be decisive and if it is not well designed the composite can be a weak or not resistant to the environment and the parts produced from it could not be used. So the aim of this thesis was to study this phenomenon of the interphase and to modify the surface of the alumina particles using different surface modifications in order obtaining the material that has improved mechanical properties.

The alumina particles were used in material reinforcement for a long period of time as they have high hardness when they have the crystal form of corundum. On the other hand, there are several other forms of alumina that have different crystal structures and that could be used both as absorbers, catalysts and reinforcements in composites. Those forms of alumina can be surface modified and further their compatibility with the polymer matrix could result in the improved materials.

Experimental part of this thesis is focused on the production and improvement of composite materials. The aim of this thesis was to show that modified alumina particles can serve as good reinforcement for composite film production and to produce the bulk material having improved mechanical properties. Production engineering is a combination of manufacturing technology, engineering sciences. “A production engineer typically has a wide knowledge of engineering practices and is aware of challenges related to production” [2]. So the possibility to fine tune the properties of a composite material and enable different uses of it in several possible fields of engineering are on the edge of production engineering and materials science showing how those two can work together in creating new materials for new uses.

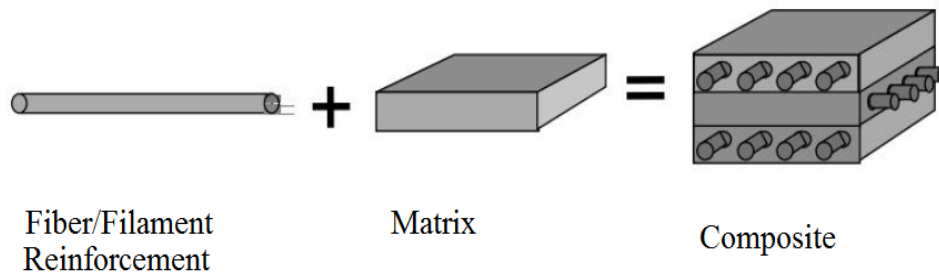
## 1. COMPOSITES MATERIALS

The composite material is made of two or more materials that combine together with a distinctive interface between them. Each material preserves its own properties but has an interaction with the other material and therefore the interface. The materials forming the composite could be ceramics, metals, and polymers.

According to the way the components are made, the resulting material may contain all the properties of the components or be significantly different from the individual components. Consequently, the resulting composite materials can obtain structural properties that exceed the individual constituent materials due to load sharing.

Composite materials are accompanying the human civilization from the very beginning of their existence. A lot of widely used materials in antiquities are composite by their structure. One of the first composite materials are the first traces of pottery that use the clay as a matrix but the pieces of rocks are taken with the clay and they form together with the material [3]. The Egyptians and Mesopotamians settlers were among the first People that used the composites by mixing clay and straw together to create strong and solid buildings, where it dates back to the year 1500 BC .Straw was used as reinforcement for composite products such as boats and pottery [4]. The objective of a composite design is achieving a set of properties that are not displayed by any single material, and also to use the best properties for each of the constituent materials. Most composites were made to improve mechanical properties such as toughness, stiffness, and high-temperature strength. Many composite materials are consisting of only two phases; one is called the matrix, which is continuous and surrounds the other phase, usually called the dispersed phase. There are a large number of composite types represented by different groups such as metals, polymers and ceramics [5].

Figure 1 shows the constituent of the composite.



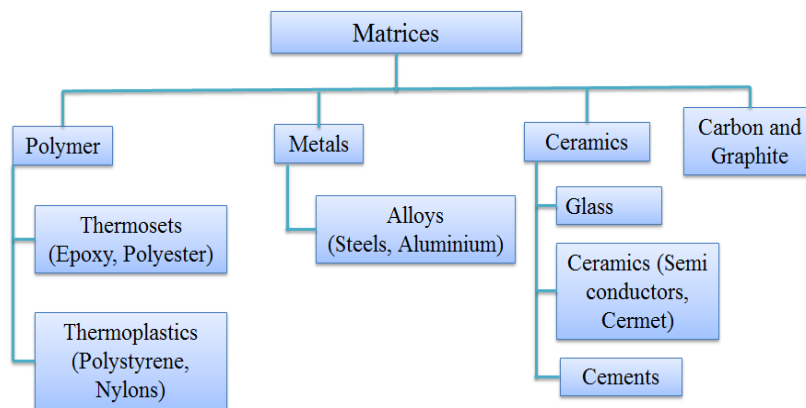
plastic, and these composites are usually called reinforced plastics. There are other types of matrices, such as metals or ceramics, but plastics are the most common used [8, 9].

### Matrix Materials

The matrix is the homogeneous material in which the reinforcement is incorporated, and it is fully continuous. This means that there is a path across the matrix to any point in the material, as opposed to two materials trapped together. In basic applications, the matrix is generally a lighter metal, for example, aluminium, magnesium, or titanium, and gives agreeable support to the reinforcement. Commonly the cobalt and cobalt-nickel alloy matrices are used in high-temperature applications [10]. In natural composites like wood, the matrix serves to unite the load-bearing fibers made of cellulose and thus, lignin binds the fibers together enabling the functioning of material from ancient times to nowadays [11].

### 1.3 CLASSIFICATION BASED ON MATRIX

The major composite classes include polymer-matrix, metal-matrix, ceramic-matrix and carbon-matrix composites. The following Figure 2 helps to classify matrices.



**Figure 2. classifications of matrices**

#### 1.3.1 Polymer Matrix Composites (PMC)

Polymers are the most generally utilized matrix materials. Polymers represented familiar plastic and rubber materials.

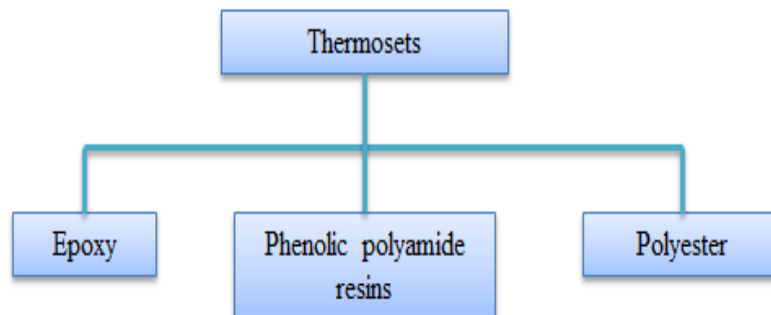
A considerable lot of them are organic compounds that are chemically based on carbon, hydrogen, and other non-metallic elements (viz. Oxygen, Nitrogen, and Silicon). Besides, they have large molecular structures, frequently chain-like in nature that has a backbone of carbon atoms [5].

Two main kinds of polymers are thermosets and thermoplastics.

### 1.3.1.1 Thermosetting Resins:-

Thermosets contain properties such as a good-bonded three-dimensional molecular structure after curing. Decompose rather than melt while heating. Simply changing the basic structure of the resin is enough to change the conditions appropriately for curing and determine its other properties. They can be kept in a partially cured state over long periods of time, making the thermosets very flexible. Therefore, they are more suitable as matrix bases for advanced conditions fiber reinforced composites. The thermosets have extensive applications in the chopped fiber composites formed especially when a premixed or moulding compound with fibers of specific quality and aspect ratio occurs to be starting material as in epoxy, polymer and phenolic. Polyesters phenolic and Epoxies are the two important classes of thermoset resins [12,13,14].

Figure 3 shows some kinds of thermosets.



**Figure 3. Kinds of thermosets**

### **1.3.2-Epoxy**

Epoxy is a polymerizable thermosetting resin and is obtainable in a variety of viscosities from liquid to solid. There are many diverse types of epoxy, and the technician must use the maintenance manual to determine the correct type for a specific repair. Epoxies are used widely in resins for preparing materials and structural adhesives. The advantages of epoxies are ease of processing, excellent adhesion, high strength and modulus, low shrinkage, low levels of volatiles, and good chemical resistance.

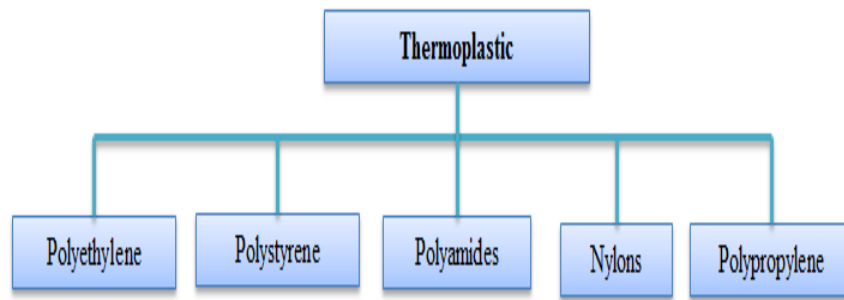
Their main disadvantages are brittleness and the reduction of properties in the presence of moisture. The curing and processing of epoxies are slower than polyester resins. The techniques processing include autoclave molding, filament winding, press molding, vacuum bag molding, pultrusion, and resin transfer molding. Curing temperatures range from room temperature to approximately 180 °C. The most common cure temperatures range between 120–180 °C [15].

**2. Polyester resins** are relatively cheap and fast processing resins and generally used for low cost applications. Low smoke producing polyester resins are used to produce the interior parts of the aircraft. Fiber-reinforced polyester can also be processed in many ways. Common processing methods contain matched metal molding, wet layup, filament winding, press molding, injection molding, autoclaving, and pultrusion [15]

#### **1.3.1.2 Thermoplastic Resins:-**

Thermoplastics have a single or two-dimensional molecular structure, tend to high temperature and show high melting point. Also, the process of softening at high temperatures can be reversed to restore its properties during cooling [16].

Figure 4 shows some kinds of thermoplastics



**Figure 4. Kinds of thermoplastics**

The advantages of thermoplastics systems over thermosets are that there are no chemical reactions, which often leads to release gases or heat. The manufacturing process is limited by the time required for heating.

There is a little option for increasing the heat resistance of thermoplastics. Adding fillers raises heat resistance. But at high temperatures, all thermoplastic composites tend to lose their strength

However, their redeeming qualities such as rigidity, toughness and ability to repudiate creep, place thermoplastics in the significant composite materials bracket. They are used in electronic products encasement, automotive control panels etc. [17].

**Table 1 the different types of thermosets and thermoplastic resins**

<b>Thermosets</b>	<b>Thermoplastics</b>
Phenolics & Cyanate ester	Polypropylene
Polyesters & Vinyl esters	Nylon (Polyamide)
Polyimides	Poly-ether-imide (PEI)
Epoxies	Poly-ether-sulphone (PES)
Bismaleimide (BMI)	Poly-ether -ether-ketone (PEEK)

### 1.3.2 Metal Matrix Materials

Most metals and alloys can be used as matrices and they need reinforcement materials that must be stable at temperature range and also non-reactive. They can withstand high temperature in a corrosive environment than polymer composites. The melting point,



mechanical, and physical properties of the composite at different temperatures determine the service temperature of composites. Most metals, ceramics and compounds can be used with matrices alloys of low melting point. The selection of reinforcements becomes more weakly with an increase in the melting point of matrix materials [18, 19]

### **1.3.3 Ceramic Matrix Materials (CMM):**

Ceramics can be described as solid materials that showing very strong ionic bonding in general and in some cases covalent bonding. High compressive strength, good corrosion resistance, high melting points, and stability at elevated temperatures, make ceramic-based matrix materials a preferred for applications requiring a structural material that doesn't leak at temperatures above 1500°C. Surely, ceramic matrices are the best option for high temperature applications.

The ceramics possess high modulus of elasticity and low tensile strain, which, have combined to cause the failure of attempts to add reinforcements to improve strength. Also at the stress levels at when ceramics rupture, there is no enough elongation of the matrix that withstands composite from transferring an effectual amount of load to the reinforcement and the composite may fail except if the percentage of fiber volume is high enough. Material is a reinforcement to benefit from the higher tensile strength of the fiber and to produce an increase in load bearing capacity of the matrix. Addition of high-strength fiber to a weaker ceramic has not always been successful and the resulting composite has often proved weaker. Where the ceramics have a higher thermal expansion coefficient than the reinforcement material, the resulting composite is not probably to get a higher level of strength. In this case, the composite will create strength inside the ceramic at the time of cooling, which leads to microcracks expanding from fibers to fibers inside the matrix. The presence of microcracking in the composite leads to a lower tensile strength than that of the matrix.[19, 20].

### **1.3.4 Carbon Matrices**

Carbon-carbon composites have attracted special attention in the military, industry, aeronautics and space industries due to their high heat of ablation and able to keep strength at high temperatures, as well as high thermal shock resistance [21,22]

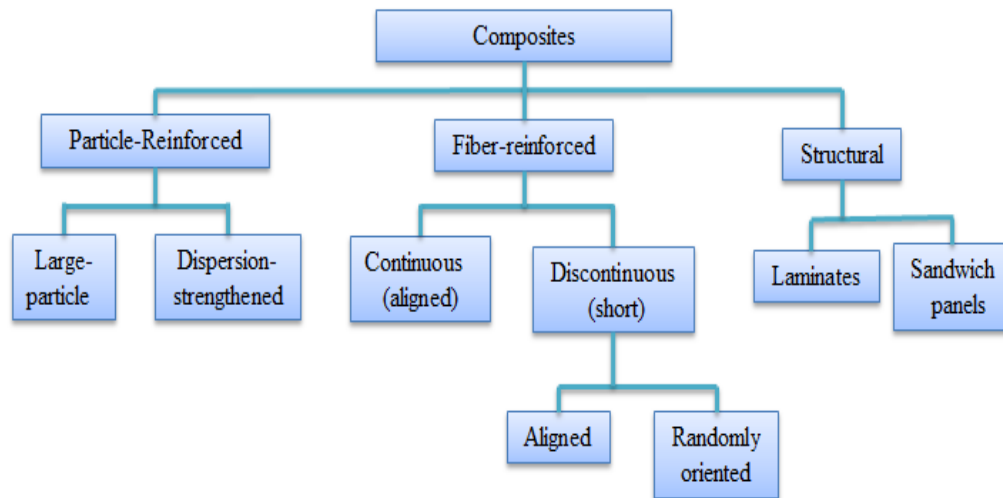
Carbon and graphite have a Featured place in composite materials choices, both being extremely superior, high temperature materials with strengths and rigidity which are not affected by temperature in the range of 2300°C.

The carbon-carbon composite is produced by the pressure of carbon or multiple impregnations of porous frames with liquid carbonise precursors and subsequent pyrolyzation. They can also be produced by chemical vapour deposition of pyrolytic carbon. The components, which are subjected to a higher temperature and on which the demands for high standard performance are many, are usually used carbon-carbon composites [23]

### **1.4 CLASSIFICATION BASED ON REINFORCEMENT**

The reinforcement is usually stronger and stiffer than the matrix and provides the composite of its good properties. Reinforcements essentially come in three forms: particulate, continuous and fiber discontinuous fiber. The particles have almost equal dimensions in all directions, although it does not must be spherical. Grains, resin powder and small balloons are examples of particle reinforcements. Reinforcements are known as fibers when one dimension becomes longer than the others. Discontinuous reinforcements (chopped fibers, milled fibers, or whiskers) are different in length from a few millimetres to a few centimetres [13].

The classification of composite materials is shown in Figure 5



**Figure 5. Schematic representation of composite materials classification**

### 1.4.1 Particle-Reinforced Composites

Microstructures compositions of metallic and ceramics composites that show particles of one phase dispersed in the other are known as particle reinforced composites. Circular, triangular, and square shapes of reinforcement are known, but the dimensions of all their sides are fairly equal. The volume of dispersion in particle composites is in order of a few microns and volume concentration more than 28%. The particles composites strengthen the system by the hydrostatic coercion of fillers in matrices and by the hardness that related to the matrix. Imparts least anisotropic property to composite particles are used to increase the modulus of the matrix, to decrease the ductility of the matrix, to decrease the permeability of the matrix. The strength of a composite is generally based on particle diameter, interparticle spacing, and volume fraction of reinforcement. The properties of the matrix affect the behaviour of the composite particles [23,24].

There are generally two types of PRC:

1. Large particle
2. Dispersion-strengthened

### 1.4.1.1 Large-particle composites

An example of a large particle composite is concrete that is consisting of cement (matrix), sand and gravel (particles). Large particle composites have been used with all three types of materials (metals, polymers and ceramics). cermets are examples of ceramic-metal composites. The cemented carbide is the most common cermet which is composed of very hard particles of a refractory carbide ceramic such as titanium carbide (TiC) or tungsten carbide (WC) which is included in a metal matrix such as nickel or cobalt. These composites are widely used as cutting tools for composites steel. Solid carbide particles supply cutting surface but are very brittle and cannot withstand the stresses of cutting. Toughness is enhanced by included in the ductile metal matrix that isolates the carbide particles from each other to prevent particle crack propagation. Each matrix and particulate phases are fully refractory, to withstand the high temperatures resulting from the cutting tools on the hard materials [5]. There is no single material can provide a set of properties possessed by Cermet. Relatively large volume fractions of the particulate phase can be used, often more than 90 vol% thus the abrasive action is maximized of the composite. Both Plastics and elastomers are usually reinforced with different particulate materials. To achieve the efficiency enhancing effect the particles must be small, correctly distributed and of uniform size. While the best engineering properties of strong particles are used in this way, the effect of brittleness is mitigated by the presence of a ductile matrix that connecting them together. The elasticity coefficient of the particle complex usually follows the rule of the mixture. It is devalued between the higher value and the lower value given by the equation [5].

Mixture rule: equation predicts that the elastic modulus must be fall between an upper and lower bound as shown

$$E_c(u) = E_m V_m + E_p V_p$$

$$E_c(l) = \frac{E_m E_p}{V_m E_p + V_p E_m}$$

Where:

$E_c$ : elastic modulus of composite

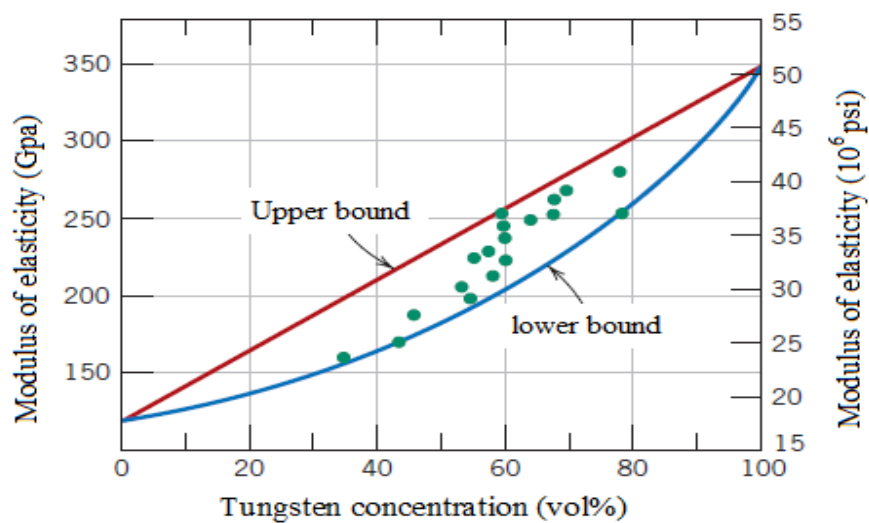
$E_p$ : elastic modulus of particle

$E_m$ : elastic modulus of matrix

$V_m$ : volume fraction of matrix

$V_p$ : volume fraction of particle

Figure 6 plots upper and lower bound  $E_c$  – versus  $V_p$  curves for a copper-tungsten composite; in which tungsten is the particulate phase.



**Figure 6. “Modulus of elasticity versus volume percent tungsten for a composite of tungsten particles dispersed within a copper matrix” [25].**

“The usage of many of the modern rubbers would be strictly restricted without reinforcing particulate materials such as carbon black. Carbon black has very small and spherical particles, mainly produced by the combustion of natural gas or oil in an atmosphere which contains only limited air supply”. By the addition of vulcanized rubber, this cheap material will enhance tensile strength, tear, toughness, and abrasion resistance.

Automobile tires have between 15 to 30 vol% of carbon black. In order for carbon black to provide significant reinforcement, the particle size should be quite small, with diameters between 20 and 50 nm; also, the particles must be equally distributed throughout the rubber and must form a strong adhesive bond with the rubber matrix. The

reinforcing of particles using other materials (such as silica) less effective because this special interaction between the particle surfaces and rubber molecules does not found [5].

#### **1.4.1.2 Dispersion-strengthened**

Strengthened of dispersion means strengthening of materials where they are in the very small particles of a hard and inert phase are uniformly dispersed within load bearing matrix phase.

Metals and metal alloys can be hardened and strengthened through the regular dispersion of several volume percentages of fine particles of extremely hard and inert material.

The dispersed phase could be metallic or non-metallic; oxide materials are usually used. The strengthening mechanism includes interactions between the particles and dislocations through the matrix, as with precipitation hardening. The strengthening is maintained at high temperatures and for long periods of time because the dispersed particles are selected to be non-interactive with the matrix phase [5]. For precipitation-hardened alloys, the increase in strength may vanish at heat treatment as a result of precipitate growth or degradation of the precipitate phase. The strength of high-temperature nickel alloys can be significantly improved by adding 3% of ThO<sub>2</sub> as finely dispersed particles. this material is called as thoria-dispersed (or TD) nickel. Same influences occur in the aluminium and aluminium oxide system. An extremely thin and cohesive alumina coating is formed on the surface of very small aluminium (0.1 to 0.2µm thick) flakes of aluminium that are dispersed in an aluminium metal matrix. These materials are called sintered aluminium powder (SAP) [5].

#### **1.4.2 Fiber reinforcement**

Fibers are the important layer of reinforcements because they meet the desired conditions and the transport strength to the matrix constituent affecting and enhancing their desired properties. There are organic and inorganic fibers used to reinforce composite materials. Nearly all organic fibers have low elasticity, density, and flexibility. Inorganic fibers have a high modulus, high thermal stability and have greater rigidity than organic fibers and in

spite of the various advantages of organic fibers which render the composites in which they are used [15].

Glass fibers are the first known fiber used in the reinforcement of materials, and then ceramic and metal fibers were discovered and widely used, to make composites stiffer and more resistant to heat. Fibers reduce performance due to several factors. The fiber composite performance is judged by its shape, length, orientation, fiber composition and mechanical properties of the matrix. The fiber orientation in the matrix is an indicator of the strength of the composite, and the strength is greater along the longitudinal direction of the fibers. That does not mean the longitudinal fibers take the same amount of load regardless of the direction in that it is applied. The best performance from longitudinal fibers could be received if the load is applied along its direction. The slightest shift in the angle of loading may significantly reduce the composite strength. Unidirectional loading is found in few structures and hence it is wise to give a mixture of orientations for fibers in composites particularly when the load is expected to be the heaviest.

Single-layer tapes that are made of continuous or discontinuous fibers could be oriented unidirectional accumulated into plies containing layers of filaments also oriented in the same direction. At the present time, computers are used to set expectations for such variations to suit special needs. Also, in flat composites, strength can be changed from unidirectional fiber oriented composites which produce in composites with approximately isotropic properties. Properties of angle-ply composites that are not the same isotropic maybe differ with the number of plies and their orientations. Composite variables in such composites are supposed to have a fixed ratio and the matrices are believed comparatively weaker than the fibers. Thus, the fiber strength in any of the three axes is one third of the unidirectional fiber compound, assuming that the percentage of the volume is equal in all three axes. Nevertheless, the orientation of short fibers in different ways is also possible, such as random orientation by spraying to a certain level or adding a matrix in liquid or solid state before or after the fiber deposition. Also, three-dimensional orientations can be achieved in this way. There are several methods of random fiber orientations, which is a two-dimensional one, yield composites with one-third the strength of a unidirectional fiber-stressed composite, in the direction of fibers. Thus a 3-dimension, this will result in

a composite with a similar ratio, about less than one-fifth. Longitudinal strength can also be calculated on the proposition that fibers have been minimized to their efficient strength on approximation value in composites with strong matrices and non-longitudinally orientated fibers. Needless to say, fiber composites can be constructed with continuous or short fibers. Experience has indicated that continuous fibers (or filaments) show better orientation; despite it does not reverse on their performance. Fibers contain a high width ratio, which means that their lengths are several times larger than their effective diameters. This is the reason why using continuous filaments in the manufacturing process. The mass production of filaments has corresponded to many matrices in various methods such as twisting, winding, knitting and weaving, which show the characteristics of the fabric. Since they have high strength and low density fiber lengths in filaments or other fibers have a significant impact on mechanical properties and also the response of composite materials for procedures and processing. Shorter fibers with suitable orientation composites which use ceramic, glass or multi-purpose fibers can have higher strength than those that use continuous fibers [26].

### **1.4.3 Laminar Composites**

Laminar composites are presented in many combinations such as the number of materials. They have been described as materials containing layers of materials bonded together. Maybe contain of many of layers of two or more metallic materials coming alternately or in a specific order more than once, and in numbers greater than the number required for a specific purpose. Sandwich and clad laminates have many areas as they should be, though they are known for following the base of standard mixtures. Other basic values related to metal-matrix, metal-reinforced composites are also well known. Powder metallurgical processes such as roll bonding, hot pressing, brazing, diffusion bonding etc., used to manufacture various alloys of foil, sheet, powder or sprayed materials. Coated metals are suitable for denser environments that require denser faces. There are many collections of foils and sheets that work as adhesives at low temperatures. Like plastics, materials or metals can be used with a third component. The best known metal-organic laminate is pre-finished or pre-painted metal which main advantage is the elimination of final finishing

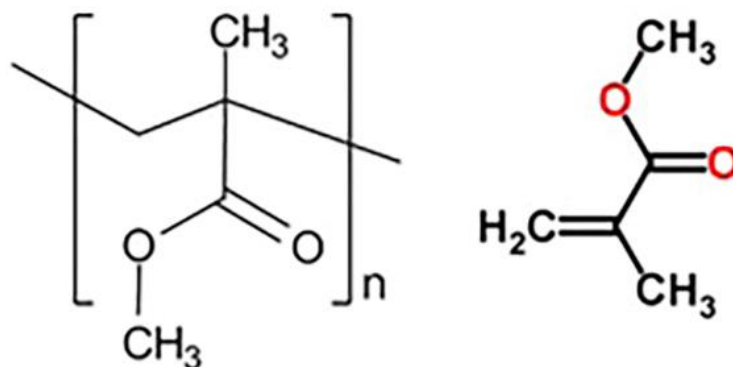


by the user. Diverse combinations of metal-plastic, laminates, vinyl-metal, organic films and metals, represent up to 95% of the known metal-plastic laminates profiles. They are made through bonding operations [27].

## **2. POLYMETHYL METHACRYLATE PMMA**

Poly (methyl methacrylate) (PMMA), also known as acrylic, acrylic glass, or plexiglass as well as by the trade names Crylux, Plexiglas, Acrylite, Lucite, and Perspex. The first acrylic acid was created in 1843. Methacrylic acid, derived from acrylic acid, was formulated in 1865. The reaction between methacrylic acid and methanol results in the ester methyl methacrylate. Polymethyl methacrylate was discovered in the early 1930s at Imperial Chemical Industries (ICI) in England by British chemists Rowland Hill and John Crawford [28].

PMMA or acrylic is a strong and lightweight material. PMMA has Chemical formula  $C_5H_8O_2$ . Acrylic density ranged between 1.17-1.20  $g/cm^3$  that is less than half the density of glass. The impact strength of PMMA is greater than that of glass and polystyrene. Acrylic can transmit up to 92% of visible light with just 3mm of thickness. With a refractive index of 1.4905 at 589.3 nm, it can reflect up to 4% light from its surface. Due to the environmental stability of acrylic better as compared to polystyrene and polyethylene it is considered used for most of the outdoor applications in the plastics industry [29].



**Figure 7. Structural formula of Polymethyl methacrylate PMMA [30]**

### **2.1 Applications of Polymethyl methacrylate PMMA.**

Polymethyl methacrylate PMMA is one of the most used thermoplastic polymers in the biomedical, optical, solar, nanotechnology, viscosity, sensors, molecular separators, polymer conductivity, battery electrolytes, and pneumatic actuators [31].

It is one of the most common types of thermoplastics because of its physical and mechanical properties, such as scratch resistant, it shows good dimensional stability, low moisture and water absorption capacity, high Young's module and hardness [32,33].

Due to its good properties such as high biocompatibility and low toxicity, manipulation, easy formation, weak absorption of visible and UV light, good corrosion resistance, relatively low cost and high endurance, PMMA is used in dentistry [34]. For dental use, PMMA should be sufficiently chewable, robust, wear resistant, shockproof and stable under thermal and mechanical load [35]. However, the material has poor mechanical strength when used alone and its main problem [36,37].

### **2.2 Production Methods of Poly (methyl methacrylate) (PMMA)**

PMMA can be produced using a variety of polymerization mechanisms. The most common technique is the free radical polymerization of MMA. Radicals can be generated with radiation, heat, or chemical agents (usually associated with radiation or heat). MMA can be polymerized spontaneously with heat. This polymerization is very slow but has no industrial relevancy. MMA has been polymerized anionically. Anionic polymerization is

not used industrially because the monomer must be very pure, and polymerization has to be done at very low temperatures. Free radical polymerization of MMA is the predominant industrial mechanism for producing PMMA [38,39].

### **2.2.1 Radiation Initiated Polymerization of MMA**

The polymerization of MMA can be initiated with light or  $\delta$ -radiation. The photoinitiation of MMA can be performed using ultraviolet UV or visible light without sensitizers. It is still not quite clear whether photoinduced polymerization is done by a free radical mechanism or by an excited state mechanism [40].

The light induced polymerization is considered one of the most efficient technologies for the rapid production of polymeric materials with well-defined properties, especially for cross-linked polymer networks. Photopolymerization is often the preferred method for rapid polymerization. Most photosensitive resins used in industrial photopolymerizations are made of acrylates instead of methacrylates, because of the very higher reactivity of the acrylate double bond. The propagation rate constant,  $K_p$ , is about 15,000 L/mole•second for acrylate monomers, that compares to less than 1,000 L/mole•second for methacrylate monomers [41].

PMMA can also be produced by initiating radiation, usually from a  $^{60}\text{Co}$  source, and electronic beams.  $\gamma$ -Radiation initiated polymerization is useful when the addition of the initiator is undesirable, or if the polymerization batch absorbs light strongly, due to the pigments or because the monomer is impregnated with porous materials, such as wood or stone [38].  $\gamma$ -Radiation is also used for sterilization purposes.  $\gamma$ -Radiation may be the polymerization mechanism of choice for polymers which must also be microbially sterile.

### **2.2.2 Heat Initiated Polymerization of MMA**

The polymerization of MMA is typically initiated by thermally labile compounds. When heating, the thermal initiator forms free radicals that initiate the polymerization.

The free radical polymerization of acrylates and methacrylates is a chain polymerization across the double bond of the monomer.

Free radical polymerizations can be done relatively easily. Unlike many types of polymerizations, absolute dryness is not necessary. For polymerization to be successful, oxygen should be completely removed from polymerization. Oxygen is a radical scavenger, terminating free radical polymerization

The free radical polymerization of MMA can be performed homogeneously, by bulk or solution polymerization, or heterogeneously, by suspension or emulsion polymerization [38,39].

### **2.2.3 Bulk Free Radical Polymerization and the Trommsdorf Effect**

In bulk polymerizations, the monomer and initiator are combined undiluted. In large batches, exotherms because the autoacceleration is a concern. The reaction rate decreases with time for most (non-radical) polymerizations. In order to polymerization of MMA and other acrylic and vinylic monomers to a high degree of conversion, especially in bulk polymerizations, the reaction rate can be controlled by the gel effect, also called the Trommsdorf effect [38,39,42]. In the first stage of the polymerization, the polymerization rate is constant or declining with time. As the polymerization progresses to the second stage, the rate of polymerization increases over time that can lead to dramatic autoacceleration known as the gel or Trommsdorf effect. In the final stage of polymerization, the third stage, the polymerization rate is constant or decreasing frequently. In bulk polymerizations, a very large increase in the viscosity of the reaction through the third stage led to hinder the diffusion of the propagating polymer radicals. Even with these viscosity and safety defects, bulk polymerizations are used commercially to produce high-gloss, optically clear acrylic glasses from MMA [38,39,42].

Bulk polymerizations of MMA remain the dominant method for production high-quality acrylic glass, such as plexiglass.

### **2.2.4 Solution Free Radical Polymerization**

Many of the bulk polymerization defects are overcome by polymerizing MMA in a solvent. The solvent acts as a diluent and helps to transfer the heat of polymerization.

Thermal control is much better in solution polymerization than in bulk polymerization. In addition, the viscosity of the reaction mixture is reduced [38,39].

The solvent should be chosen carefully. Many organic solvents act as chain transfer agents for free radical reactions, so reducing the polymer molecular weight. Aromatic solvents can accept and stabilize a free radical, in fact, leads to inhibition of polymerization [42]. For solution polymerizations of MMA, N, N-dimethylacetamide and dimethylformamide are examples of acceptable solvents.

Solution polymerizations of MMA are used commercially to produce additives, paint resins, and adhesives [38,39].

### **2.2.5 Suspension Polymerization**

Small beads of PMMA can be produced easily using suspension polymerization. The monomer is stirred about twice its volume of water and dispersants. That forms a droplet like suspension of the monomer phase in the aqueous phase. Dispersants stabilize the polymerization and prevent the droplets from adhesion to each other. Dispersants are water soluble compounds like cellulose derivatives, gelatin or water soluble polymers such as poly (vinyl alcohol). Dispersants can also be suspended inorganic compounds, such as magnesium carbonate, kaolin, or aluminium hydroxide. The size of a bead or particle can be controlled by selecting stirring conditions and suitable dispersants, to produce beads ranging from 50  $\mu\text{m}$  to 1000  $\mu\text{m}$  [38].

The suspension polymerization is initiated with free radical initiators which prefer the monomer phase, like benzoyl peroxide. The Suspension polymerization provides for the removal of heat from the polymerization by the aqueous phase, however allowing for high polymerization rates in the monomer phase. After completion of the polymerization, the PMMA polymer beads can be easily separated from the aqueous phase by filtration, washed with water, and dried [38].

Suspension polymerizations of MMA produce PMMA beads, which can then be molded [38,39].

#### **ADVANTAGES**

- The polymer can be easily recovered by filtering the beads.

- Water is commonly used as a medium: inexpensive, good heat transfer, environmentally friendly.
- Viscosity is not a problem.
- The size of the bead can be controlled.

## **DISADVANTAGES**

- Can be used effectively only for glass materials (not low Tg materials)

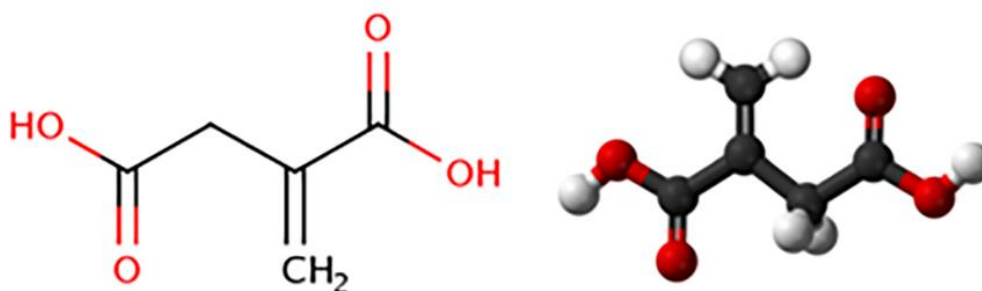
### **2.2.6 Emulsion Polymerization**

The emulsion polymerization is used to make colloidal dispersion of PMMA. Emulsion polymerization includes free radical polymerization of the monomers which are in the colloidal suspension. Surfactants are usually added to the aqueous phase to form micelles. The free radicals initiators used are soluble in water, like potassium persulfate. Monomer, including a fraction of free radical initiated monomer, migrates to the micelles. Inside the micelles, the concentration of the monomer is extremely high, and this is where polymerization occurs. In ideal conditions, theoretically, there is one propagating chain end per micelle. The emulsion polymerization provides for high conversion and extremely high molecular weight polymer within the micelles. The dispersed particles of PMMA produced are extremely small, ranging from 0.001  $\mu\text{m}$  to 0.100  $\mu\text{m}$  [39,42].

Emulsion polymerizations of MMA are used to produce paint resins, paper coating agents and paper processing agents, textile binders, and additives [38].

### **2.3 Itaconates**

Itaconic acid and itaconates are preferred materials for environmentally friendly applications, as they are not produced from petrochemical sources, but from plant products [43]. Itaconic acid was first described by Baup in 1836 when he discovered it as a product of citric acid distillation. Itaconic acid has the stoichiometric formula  $\text{C}_5\text{H}_6\text{O}_4$  and a molar weight of 130.1 g/mol. It exists as white to light beige crystals with a density of 1.573 g/mL at 25 °C, a melting point of 165-168 °C and a flashpoint of 268 °C [44]. Dissolves in water up to 80.1 g/L at 20 °C which makes it extremely easy to purify by crystallization [45].



**Figure 8. Structural formula of itaconic acid [46].**

Itaconic acid is structurally quite similar to methacrylic acid, excepting that at the  $\alpha$ -carbon atom a carboxyl group is attached instead of the H atom. Though the price of itaconic acid is higher than methacrylic acid, however, itaconic acid and itaconates are more acceptable in terms of the environment because itaconic acid is obtained from plants (mainly by enzymatic transformations of molasses), whereas methacrylic acid gets from petrochemical sources [47, 48]. As a dibasic acid, itaconic acid offers more options when comparing its esters with methacrylic acid. Since there are many similarities in itaconates with the corresponding methacrylates and the advantages mentioned, it represents an interesting alternative to methacrylates in the synthesis of a variety of materials.

Itaconic acid is also readily biodegradable in nature. Itaconic acid is valuable as a monomer because of its unique chemical properties that derived mainly from its methylene group and its possession of two carboxylic acid groups. Itaconic acid is able to participate in addition to polymerization, which gives polymers with many free carboxyl groups that give beneficial properties to the polymer. It can either be self-polymerised or can act as a co-monomer with other monomers to form heteropolymers [49]. Itaconates have been widely used in various medical applications because of their extremely low toxicity [50]. In addition, itaconic acid and its derivatives are widely used in the preparation of paints and coatings [51, 52] composite resins [53, 54] contact lenses [55] and products for personal care [56]. It has been shown that the addition of itaconate led to a decrease in water absorption and significantly reduced the residual methyl methacrylate content [57].

## 2.4 Alumina $Al_2O_3$

Alumina ( $Al_2O_3$ ) or aluminium oxide is a chemical compound of aluminium and oxygen, exists in nature as the mineral corundum ( $Al_2O_3$ ); diaspore ( $Al_2O_3 \cdot H_2O$ ); gibbsite ( $Al_2O_3 \cdot 3H_2O$ ); and most commonly as bauxite [58]. There are many forms of  $Al_2O_3$  crystalline structures, such as ( $\chi$ -,  $\eta$ -,  $\delta$ -,  $\kappa$ -,  $\theta$ -,  $\gamma$ -,  $\rho$ ) besides the thermodynamically stable  $\alpha$ - $Al_2O_3$  (corundum). The stability and the high elastic modulus of corundum made it one of the most used materials in high temperature applications.

The extraordinary chemical properties of alumina have been used in composites materials for many years as reinforcement [59, 60] and as a catalyst in many chemical reactions [61] adsorbent in analytical chemistry [62], as well as material for high-temperature applications [63].

Aluminium oxide (alumina;  $Al_2O_3$ ) is a typical engineering ceramic material possesses advantages such as its thermal, chemical and physical properties when compared to many ceramic materials. It is widely used in the manufacture of bricks, abrasives and integrated circuit packages (IC) [64].

### 2.4.1 Production Methods of Alumina $Al_2O_3$

$Al_2O_3$  nanoparticles can be synthesized by many different methods, such as the hydrothermal [65] precipitation [66], sol-gel processing [67–69] reverse microemulsion [66,70], thermal decomposition [71], flame spray pyrolysis [72] and combustion method [73].

However, descriptions of the preparation of  $Al_2O_3$  nanoparticles by using water-in-oil microemulsion were limited [74].

The method of co-precipitation and sol-gel has been used to prepare metal oxide or composite metal oxide by chemical reaction. In fact, their advantages lie in putting the homogeneous mixture of different components into practice. However, in the preparation period, an expensive alcoxide such as primary metals and more complex sampling procedures should be used, further complicating the preparation process and operating costs. The thermal decomposition of organic compounds in the organic medium is a method available to prepare inorganic materials. But this method should be performed



under certain pressure and temperature, meaning that the operating state is somewhat critical. Water-in-oil (W/O) microemulsions or reverse microemulsions technology are one of the most recognized methods because of their many advantages, for example, soft chemistry, which does not require great pressure or temperature control, ease of handling, and does not require any special use or expensive equipment, and was invented as an effective process for the preparation of nanoparticles in the 1980s [75, 76].

#### **2.4.2 Applications of Alumina $Al_2O_3$**

Aluminium Oxide (Alumina,  $Al_2O_3$ ) is one of the most versatile types of engineering ceramics due to its high temperature service limit along with its chemical, mechanical and electrical properties. It has good thermal conductivity and high mechanical strength and wears resistance [77]. Its hardness makes it suitable for use as an abrasive and as a component in cutting tools [78], remove water from gas streams [79].

The material, provides excellent electrical insulation properties, low dissipation factor, and great dielectric strength [80]. These characteristics enable the use in high voltage electrical applications.

Moreover, the chemical strength of the alumina is large. Most acids and alkalis can resist even at high temperatures.

Mechanical properties, as well as adhesion, are improved using the possibility to strengthen the interphase bonding. Silanes are synthetic hybrid organic-inorganic compounds that are used as coupling agents across organic-inorganic interfaces for bonding dissimilar materials. Silanes have been used to enhance the bonding between organic coatings/adhesives and ceramics or metals in various industries since the 1940s. In the applications in dentistry and dental technology, silanes are widely used as coupling agents to bond resins to silica-coated metals, ceramics and resin composites [81]. When bonding an acrylic resin, the hydrolyzed alkoxy groups (silanols) in silane molecules react with the hydroxyl group of the metal surface while the organofunctional group reacts with the monomeric resin matrix [82]. Historically, the silane modification of the alumina surface has been found to exhibit weak hydrolytic stability due to the large electronegativity difference between Al and Si atoms. The improvement of hydrolytic

stability of the alumina surface was achieved through the hydrosilylation that consisted of a two-step process in which the surface OH groups were first converted to hydrides that reacted with Bis-GMA/TEGDMA monomers [83].

Despite these historical findings, a two-step modification of alumina surface was accepted; first by amino silane and the second by linseed oil esters (biodiesel). The linseed oil esters have long hydrophobic chains that give the elasticity to the material and serve as protection of the alumina surface (Al-O-Si bond hydrolyze in the presence of water).

### 3. MATERIALS CHARACTERIZATION METHODS

Fourier-transform infrared spectroscopy (FTIR) was used for the characterization of the chemical composition of two different modifications of alumina-based particles and obtained composite films. Tests were performed using a Nicolet iS10 spectrometer (Thermo Scientific) in the attenuated total reflectance (ATR) mode with a single bounce 45 °F Golden Gate ATR accessory with a diamond crystal, and DTGS detector. FTIR spectra were obtained at 4 cm<sup>-1</sup> resolution with ATR correction. The FTIR spectrometer was equipped with OMNIC software and recorded the spectra in the wavelength range from 2.5 μm to 20 μm (i.e., 4000 –500 cm<sup>-1</sup>).

The morphologies of the composite with two different modifications of alumina-based particles were examined using a field emission scanning electron microscope (FE-SEM), MIRA3 TESCAN, operated at 3 kV.

The Vickers Hardness Number (VHN) was obtained using the following equation:

$$VHN = 2 \cos \frac{22^\circ P}{d^2} = \frac{1.8544P}{d^2}$$

where P (kgf) is the applied load and d (mm) is the length of the indentation diagonal [84].

The hardness of the samples was measured at the micro Vickers machine with different loads (15, 25, 50, 100, 300 and 500 g) for 25 s, whereby for each loading three indents were performed. Images of indentation marks were made by the optical microscope and

were used to obtain the diagonal lengths using the Image-Pro Plus 4.0 (Media Cybernetics) for each indent.

Adhesion of the obtained composite films on the metal surface was assessed by wetting angle determination. A drop of the composite mixtures was placed on a metal substrate and polymerized using the UV lamp. Wetting angle determination was also applied in determining the hydrophobicity of the particle surface. Substrates of the used particles ( $\text{\O}10$  mm) are obtained at 10 tons for 2 min in the Atlas manual hydraulic press 15T, Specec, UK. The images of the samples were taken with an optical microscope (Smart 5MP Pro) and the contact angles of the composite to the metal surface were determined using the image analysis software.

In order to verify the hypothesis of stabilizing the Al-O-Si bonds using the second coating by the linseed oil ester, the experiment of alumina surface stability was performed. The surface-modified particles  $\text{Al}_2\text{O}_3$  Fe-AM and  $\text{Al}_2\text{O}_3$  Fe-BD (100 mg) were dispersed in 6 ml of water in a sealed container for 48 hours at 80 °C. After completion of hydrolysis, the samples were centrifuged, dried at 60 °C for 12 h and analyzed by FTIR spectroscopy. “Thermogravimetry (TG) and differential scanning calorimetry (DSC) SDT Q600 simulated TGA-DTA instruments (TA Instruments) were used to study a thermal property of the composites. The samples were heated to 800 °C (10 °C/min) in a flow of nitrogen (100 cm<sup>3</sup>/min)” [85]

“An ultrasonic vibratory cavitation device was used for cavitation tests in accordance with the ASTM G32-92 Standard (stationary specimen method). The device consisted of a 360 W high-frequency generator, electrostrictive transducer, transformer for mechanical vibrations, and a water bath containing the test specimen. Recommended standard values [86] were used:

- frequency of vibration:  $20 \pm 0.5$  kHz
- the amplitude of vibrations at the top of the transformer: 50  $\mu\text{m}$
- the gap between the test specimen and the transformer: 0.5 mm
- the temperature of water in the bath:  $25 \pm 1$  °C
- ordinary water flow: from 5 to 10 ml/s” [86].

“The surface morphology of the composites exposed to cavitation was observed through a Mira3 Tescan field emission scanning electron microscope (FE-SEM), operated at 20 kV. The samples were previously coated with a thin gold film. The other device for investigation of the surface morphology was atomic force microscopy (AFM) with NanoScope 3D (Veeco, USA) microscope operated in tapping mode under ambient conditions. Etched silicon probes with spring constant  $20 - 80 \text{ Nm}^{-1}$  were used” [87].

# **Experimental part**

Experimental part presents the alumina particles that are one of the very important reinforcement particles used in composites. As for composites the interphase is of crucial importance the first part of the experimental part will present the synthesis, surface modification and characterization of reinforcement particles. The selected particles modifications enabled the use of those particles in thin films where they improve mechanical properties as well as adhesion to the substrate. Those particles improve also the bulk properties of materials.

The second and third part of the experimental is resulting from further studies of composite materials. The second part examines the effect of different amounts of modified particles on the adhesion estimation of UV acrylate photopolymer films on a metal substrate. The third part deals with the testing of mechanical properties and the cavitation resistance of composite materials with different amounts of modified particles.

#### **4. SYNTHESIS OF ALUMINA PARTICLES AND THEIR SURFACE MODIFICATION**

Alumina has several crystal structures that occur in different applications. Those structures depend on the previous history of preparation. So those structures have advantages in some uses and disadvantages in other. The only stable structure of alumina is the corundum or  $\alpha$  alumina structure. This structure has the very high hardness and is suitable in high temperature applications. On the other hand, low temperature structures have more open structure, are more reactive and are suitable as adsorbents or catalysts.

Hematite is a stable ferrous oxide. This structure is formed at relatively low temperature and is stable up to high temperatures. The similarity of the structures of hematite and corundum is high and ferrous oxide when added to the alumina structure provokes the formation of the corundum structure at lower temperatures.

This was the motivation to use the ferrous oxide modified alumina particles in the research used in this thesis. Two parameters were studied in the synthesis of reinforcement particles that is the addition of the ferrous oxide precursor and the use of heat treatment to optimize

the structure of the reinforcement. The addition of the ferrous oxide also has some influence of the reactivity of the particle surface.

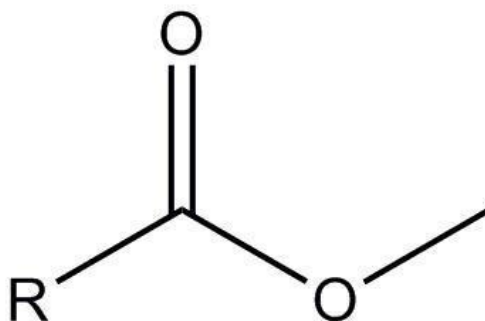
#### **4.1 Preparation of alumina particles**

Sol-gel technique was used to synthesize the alumina particles doped with  $\text{Fe}_2\text{O}_3$ . The starting materials were the:  $\text{Al}_2\text{Cl}(\text{OH})_5 \cdot 2.5 \text{H}_2\text{O}$  (Locron L),  $\text{FeCl}_3 \cdot 6\text{H}_2\text{O}$  (Sigma-Aldrich) and demineralized water. The sol was formed using the magnetic stirrer and the formation is relatively simple. The formed sol was transformed in the gel during the aging process. This process is spontaneous and takes one or two days at room temperature. The gel was heat-treated at  $900 \text{ }^\circ\text{C}$  in order to obtain a suitable crystal structure having an important part of corundum crystal structure for the reinforcement of the matrix. The amount of  $\text{Fe}_2\text{O}_3$  precursor was adjusted to obtain 10 wt. %  $\text{Fe}_2\text{O}_3$  in the final composition of particles. This amount of the ferrous oxide particles enables the solid solution creation at high temperatures as in this amount hematite is soluble in corundum.

In order to compare the synthesized alumina particles to the pure alumina particles the commercial alumina nanoparticles were used. “The alumina nanoparticles were used as received from the producer ( $\gamma$ -phase, Sigma-Aldrich, spherical alumina nanoparticles < 50 nm), denoted as ( $\text{Al}_2\text{O}_3 \text{ n}$ )” [85]. The same way of surface modification was used for those particles as for the synthesized particles.

“The particles were modified in two steps like the synthesized ones: with 3-aminopropyl tri – methoxy silane (AM) and methyl esters of linseed oil fatty acids (biodiesel – BD). The modification of the particles is described in a previous research” [88].

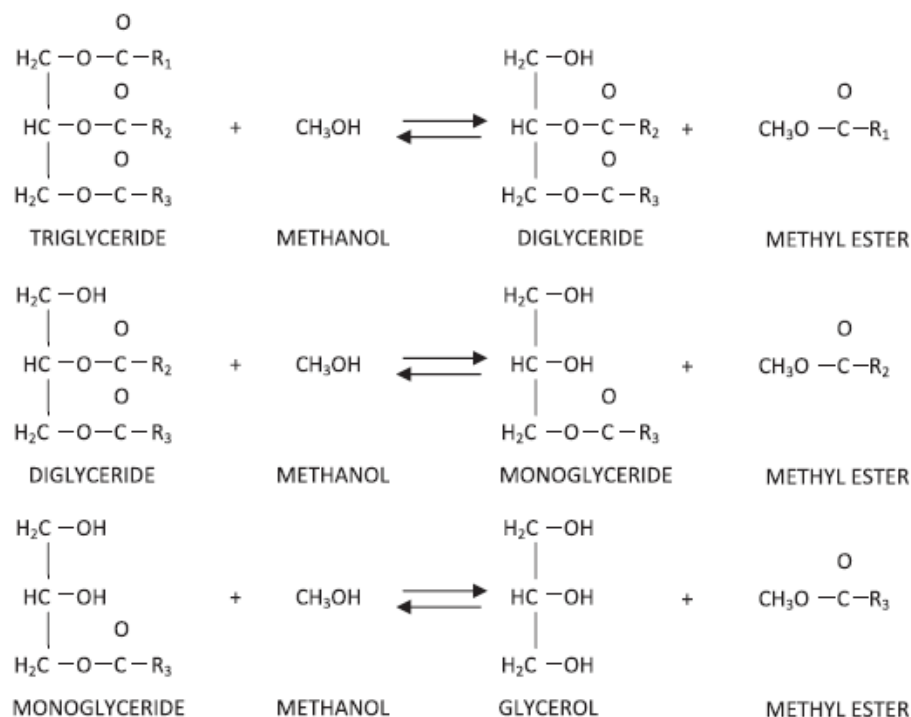
## 4.2 Synthesis of methyl ester of linseed oil fatty acid (biodiesel – BD)



**Figure 9 Methyl ester of linseed oil fatty acid (biodiesel – BD) [89].**

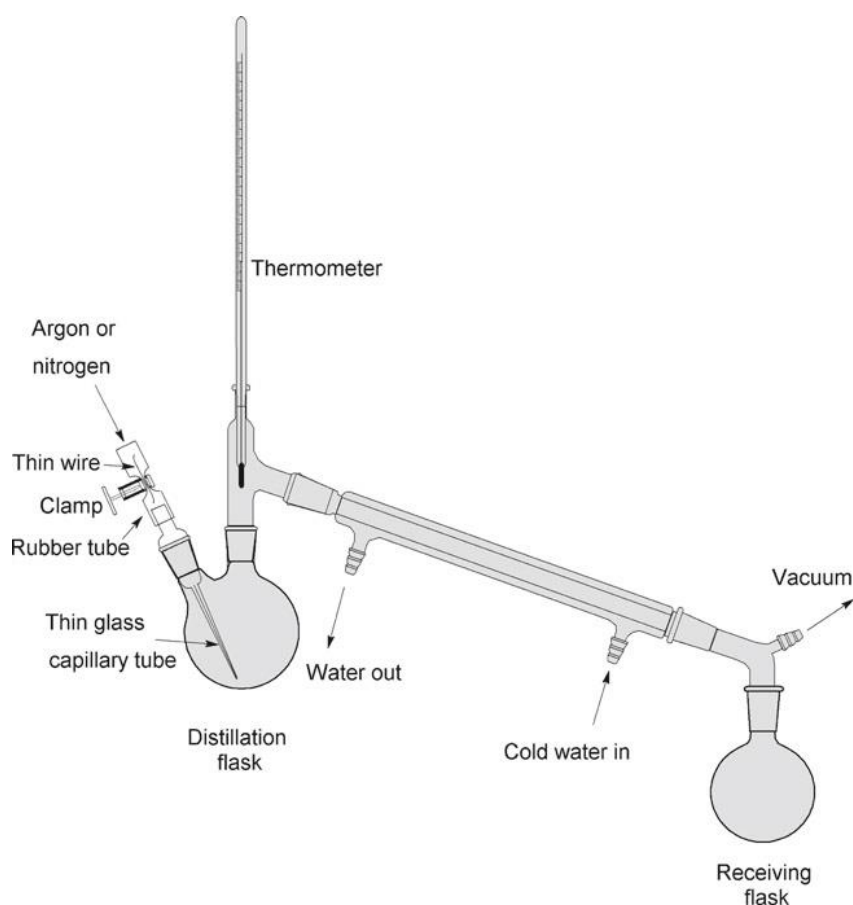
The methyl ester of the linseed oil fatty acid is a result of the research that is concentrated on the replacement of the fossil fuels by renewable sources of energy. Linseed oil has been studied for a long time and has been studied as the source of different materials that can be polymerized. This is due to the fact that this material is a triglyceride having long chains of fatty acids that contain unsaturated bonds. This make it an ideal material to be modified and to be used in different purposes [90]. The aim of this process is to extract the ester from tryglycerides and to further use them as energy source. In this thesis those products are used to modify the surface of the particles and to obtain a hydrophobic surface that will give new properties to the reinforcement that is aimed to be used in the composite material.





**Figure 10 Stoichiometry of reactions for methyl esters from triglycerides [90].**

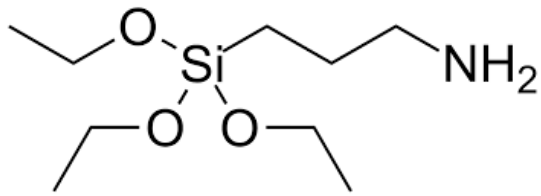
In a four-necked glass reactor of 2 l, equipped with are flux condenser, mechanical stirrer, and thermometer and dropping funnel, 929 g (3.3 mol) of linseed oil, dissolved in 85 mL of methanol, was added. The potassium hydroxide solution in methanol (0.12 mol of KOH in 102 ml of methanol) was added drop wise. Afterward, the reaction mixture was heated at 58–62 °C for 3 hours, and left to cool down. The bottom layer, *i.e.* mainly raw glycerin, was separated, and the upper layer was treated with active charcoal and filtered through diatomaceous earth. After drying with sodium sulfate, the obtained linseed oil methyl ester (biodiesel) was purified by vacuum distillation under nitrogen. Characteristics of methyl ester of linseed oil fatty acid mixture, named BD: acid value (AV) 5 mg KOH/g; ester content 97%; iodine value 152 [91].



**Figure 11 Apparatus for vacuum distillation under nitrogen [92].**

### **4.3 The first step of surface modification of alumina-based particles using 3-aminopropyl)tri – methoxy silane**

Silanes are used as the “universal” modifier and a coupling agent in a lot of situations. Their organic-inorganic nature enables them to establish bonding to the inorganic material of the reinforcement and to enable the bonding to the polymer matrix or even to enable the bonding to the other surface modifier of the reinforcement. 3-aminopropyl)tri – methoxy silane is a frequently used chemical as it has functional groups that enable good connectivity both to the inorganic particle and to the polymer matrix.



**Figure 12 The structure of 3-aminopropyl)tri – methoxy silane used as the primary modification of the surface of the alumina particles [93].**

1 g of alumina particles were dispersed in 75 ml of toluene on a mechanical stirrer in reflux under the flow of nitrogen. The mass of 1 g of silane coupling agent, 3-aminopropyl)tri – methoxy silane, (AM) was added and the reaction was time was 22 h, once the boiling point of toluene was achieved [94, 95]. The particles were filtrated and washed with hexane to remove non reacted silane after the reaction time expired. The particles were dried on 40 °C in the laboratory dryer for 12 h and then used in the preparation of composites [96]. The ferrous oxide doped alumina particles modified with AM were denoted as  $\text{Al}_2\text{O}_3 \text{ Fe} - \text{AM}$ .

#### **4.4 The second step of alumina modification with BD**

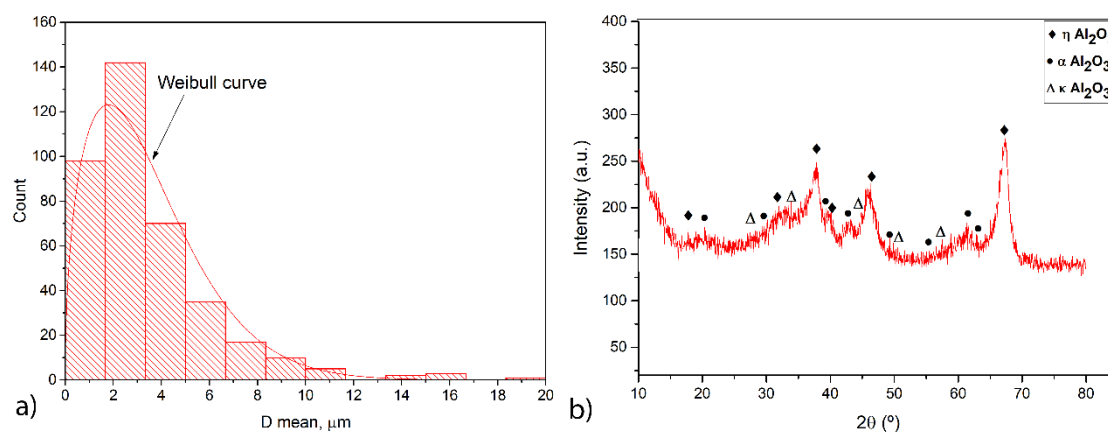
The modified alumina with a terminal amino group, from the first step of alumina modification, was dispersed in 50 ml THF and 1.56 g of methyl ester of linseed oil fatty acids were charged in a three-necked glass reactor, equipped with a magnetic stirrer, thermometer reflux condenser, and calcium chloride protection tube. The reaction took place for 12 h at 25 °C, whereupon the mixture was heated to 60 °C and maintained for 2 hours. The obtained particles were filtered under the vacuum, two times re-dispersed in THF and filtered, washed with absolute ethanol and dried at 40 °C for 12 h [97].  $\text{Al}_2\text{O}_3 \text{ Fe}$  particles modified with BD were denoted as  $\text{Al}_2\text{O}_3 \text{ Fe} - \text{BD}$ .

## 4.5. Results of particle surface modification discussion

“The diameters of the alumina based particles were determined by a particle size analyzer and were found to be:  $d(0.1) = 0.412 \mu\text{m}$ ,  $d(0.5) = 0.608 \mu\text{m}$ ,  $d(0.9) = 1.208 \mu\text{m}$  [98]. The crystal structure determined by XRD was:  $\eta - \text{Al}_2\text{O}_3$  (39.4%),  $\kappa - \text{Al}_2\text{O}_3$  (35.1%) and  $\alpha - \text{Al}_2\text{O}_3$  (25.5%)” [99], Figure 13.

### 4.5.1. XRD characterisation of particles

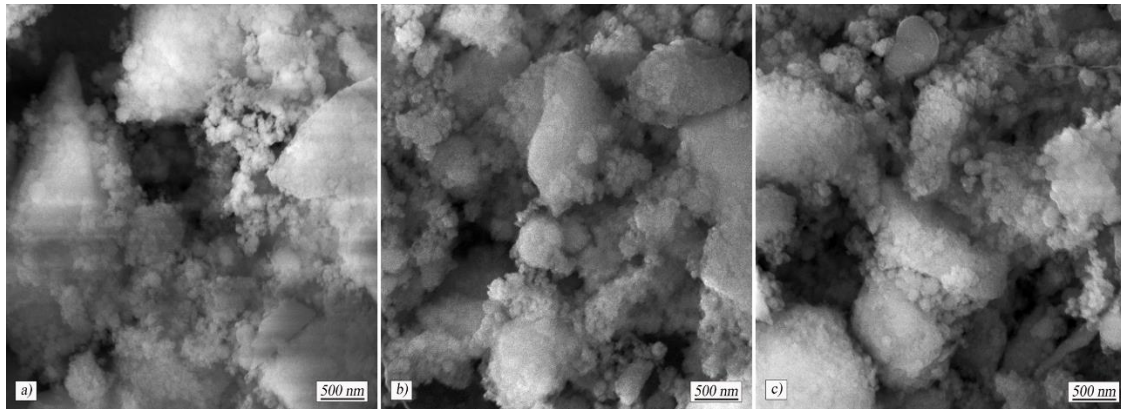
The first step in particles characterisation consists of crystal structure modification combined with the morphological characterisation



**Figure 13 a) Distribution of the diameter of synthesized ferrous oxide doped alumina particles and b) XRD of the synthesized ferrous oxide doped alumina particles after heat treatment at 900 °C [99].**

### 4.5.2. SEM characterisation of particles

The purpose of the surface modification was to prevent the agglomeration of particles. Particles that does not form clusters are easier to use in composite preparation, and they don't remain together but rather are spread into the composite structure. The addition of only the silane layer is beneficial for this purpose, but addition of an additional hydrophobic layer gives new properties to be studied. Ferrous oxide doped alumina-based particles with different surface modifications were examined using the field emission scanning electron microscope (FE-SEM), Figure 14.



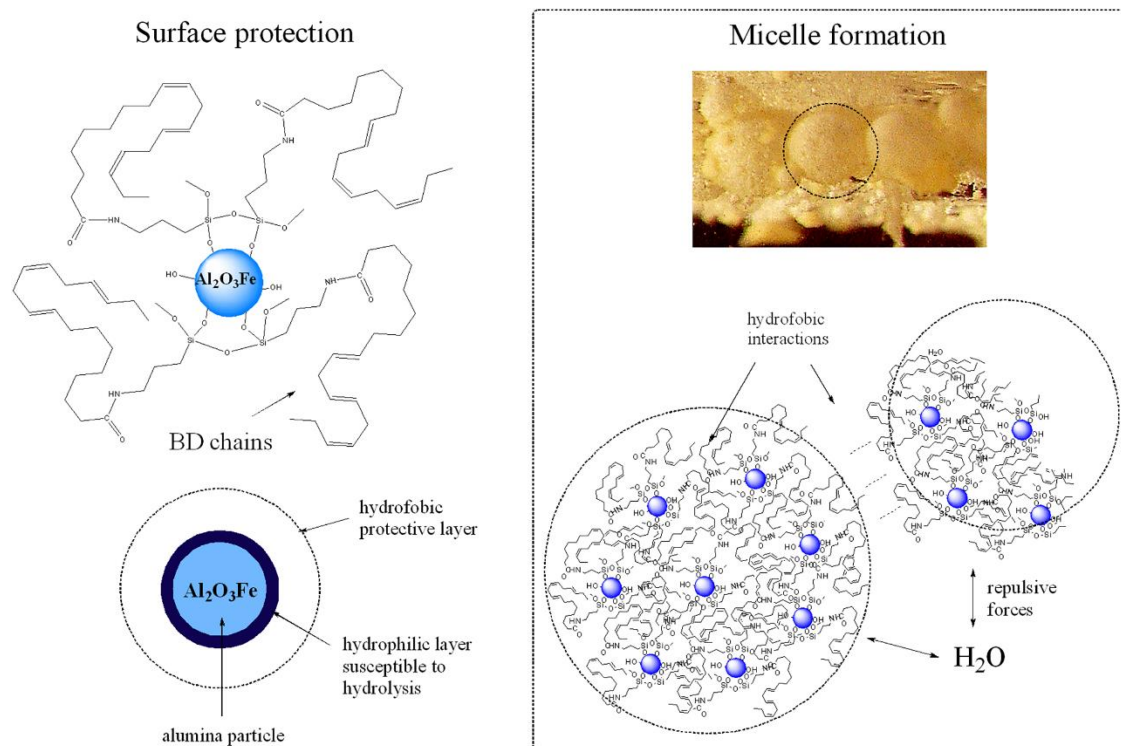
**Figure 14. FE-SEM images of the particles: a) ferrous oxide doped alumina-based particles –  $\text{Al}_2\text{O}_3$  Fe, b)  $\text{Al}_2\text{O}_3$  Fe - AM particles and c)  $\text{Al}_2\text{O}_3$  Fe - BD particles [85].**

FE-SEM images showed similar particle size and morphology before and after surface treatment, Figure 14 a-c. The particle size of  $\text{Al}_2\text{O}_3$  Fe particles was previously determined by particle size analyser and the obtained values:  $d(0.1) = 0.412 \mu\text{m}$ ,  $d(0.5) = 0.608 \mu\text{m}$ ,  $d(0.9) = 1.208 \mu\text{m}$  [100], saying that the  $\text{Al}_2\text{O}_3$  Fe particles were of submicron size. Surface modification of synthesized particles didn't significantly change the observed microstructure. Such results indicate that the low extent of cross-linking reactions between the particles, in the course of silane deposition on the alumina surface, took place. This is an important fact with the aim of achieving good dispersion of the particles and thus, the significant reinforcing effect could be achieved.

#### **4.5.3. Characterisation of the hydrophobicity of the particle surface modification**

The creation of a hydrophobic layer on the surface of the ferrous oxide doped alumina could serve as a protection of an easily hydrolyzable Al-O-Si bond is presented in Figure 15. The proposed interactions in a hydrophilic medium such as ( $\text{H}_2\text{O}$ ) are presented. Unsaturated olefin (BD) chains as a nonpolar segment on alumina particles tend to coil providing particle aggregation in an aqueous solution acting as a hydrophobic barrier to surrounding water molecules. Hydrophobic interactions are usually considered to have an entropic effect originating from the disruption of the hydrogen bonds between water molecules by the nonpolar particles considered as highly dynamic ones [101].  $\text{Al}_2\text{O}_3$  Fe-

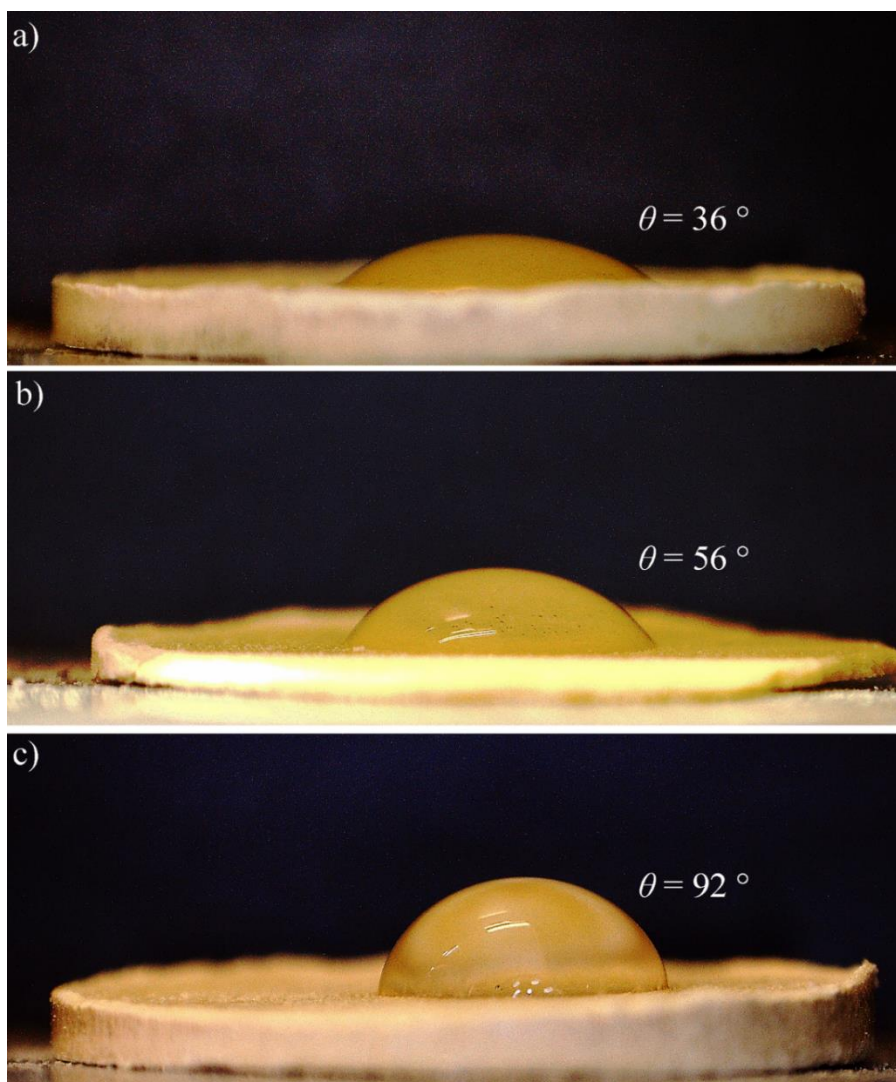
BD particles make clusters so their corresponding interface area with polar molecules is negligible.



**Figure 15. Schematic representation of surface hydrophobization and proposed interactions in a hydrophilic medium (H<sub>2</sub>O) [85].**

The wetting angle of alumina-based particles (Al<sub>2</sub>O<sub>3</sub> Fe, Al<sub>2</sub>O<sub>3</sub> Fe-AM and Al<sub>2</sub>O<sub>3</sub> Fe-BD) is presented in Figure 16. Al<sub>2</sub>O<sub>3</sub> Fe without surface modification are supposed to be hydrophilic and they showed good droplet spreading on the surface. This behaviour was explained by the presence of free hydroxyl groups on those particles surface. AM surface modification of particles introduced larger nonpolar (propyl) then polar (amino – NH<sub>2</sub>) group on the surface and thus led to somewhat increased hydrophobicity of the Al<sub>2</sub>O<sub>3</sub> Fe-AM surface. The presence of this layer enabled the particles to become partly hydrophobic. Introduction of long aliphatic groups on the surface lead to a significant change. The long aliphatic olefin chains present on the Al<sub>2</sub>O<sub>3</sub> Fe-BD surface completely made the particles hydrophobic and this is well illustrated if the contact angle is observed. Al<sub>2</sub>O<sub>3</sub> Fe-BD particles were repellent to water as a result of repulsive forces present

between the nonpolar substrate and polar water molecules. In this way the three different sorts of reinforcements were prepared, hydrophilic with no surface modification, partly hydrophobic with AM modification and finally the highly water repulsive particles having BD modification.

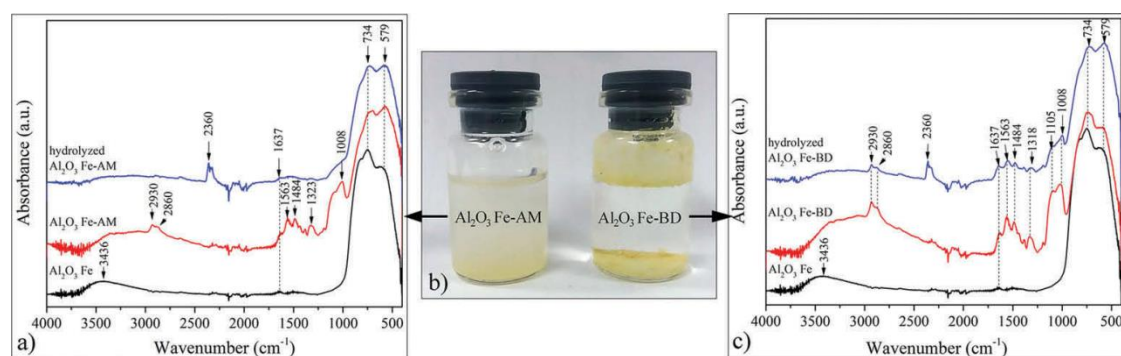


**Figure 16. Wetting angle determination with a water droplet on a substrate obtained from: a) Al<sub>2</sub>O<sub>3</sub> Fe, b) Al<sub>2</sub>O<sub>3</sub> Fe-AM, and c) Al<sub>2</sub>O<sub>3</sub> Fe-BD particles [85].**



#### 4.5.4. FTIR characterisation of particles surface modification

The FTIR is used to examine the presence of the specific chemical bonds in a specific composition. The FTIR spectra of neat  $\text{Al}_2\text{O}_3$  Fe, particles being modified with AM and particles with hydrophobic BD modifications are shown in Figure 17.



**Figure 17. Comparison of FTIR spectra of ferrous oxide doped alumina-based particles used in composites preparation and after the hydrolysis [85].**

The characteristic peaks of  $\text{Al}_2\text{O}_3$  Fe particles and particles with surface modifications (AM/BD) observed at  $3460\text{ cm}^{-1}$  can be assigned to  $-\text{OH}$  groups [102]. The characteristic peaks at  $1636/1639\text{ cm}^{-1}$  related to the  $-\text{OH}$  vibrational bending mode [103,104]. Absorption at  $\sim 734\text{ cm}^{-1}$  could be attributed to the vibrational modes associated with the  $[\text{M}^{\text{II}}, \text{III}(\text{OH})_6]^{4-,3-}$  complexes distributed along with the layered double hydroxide (LDH) layers mostly attributed to the  $\gamma$  crystalline structure of alumina [62, 105, 106].

FTIR spectra confirmed the surface modification of the prepared particles. The presence of AM/BD functionality was identified by the appearance of new peaks. The peaks at  $\sim 2935\text{ cm}^{-1}$  are attributed to the adsorption peaks of propylene C–H stretch bands of attached organic compounds, accompanied by the peaks at  $1566$  and  $1485\text{ cm}^{-1}$  from their bending vibrations. The peaks at  $1636/1639\text{ cm}^{-1}$  showed that the skeletal C=C double bond vibrations from silane functional groups were overlapped with  $-\text{OH}$  vibrational bending mode. The stretching  $\nu$  (N–H) vibrations often observed at about  $800\text{ cm}^{-1}$  (characteristic peak for AM modification) were overlapped with vibrational modes of the alumina crystal structure.



After the hydrolysis of modified particles, a doublet peak was observed at the  $\sim 2360$   $\text{cm}^{-1}$  that was attributed to environmental  $\text{CO}_2$  gas [107]. Figure 17b clearly shows the hydrophobic behavior of  $\text{Al}_2\text{O}_3$  Fe-BD particles that were resistant to the hydrolysis process of the Al-O-Si bond protected by olefin BD chains. FTIR spectrum after hydrolysis of  $\text{Al}_2\text{O}_3$  Fe-BD particles shows insignificant changes in the chemical structure of particle surface, Figure 17c. The formation of particles in the micelles (Figure 15) protected the core particles providing improved resistance to hydrolysis by water.

#### 4.5.4. TG of surface-modified alumina-based particles

Table 2 summarizes the results from TGA diagram and DTG peaks of thermal degradation of particles before, with and without surface modification. Mass residuals attributed to the alumina particles free from adsorbed water and silane coupling agents were detected by the TGA analysis. These data revealed the efficiency of the surface modifier bond to the outer surface of the ceramic. The difference in mass loss serves to calculate the quantity of the BD modifier attached to the particle surface ( $\text{Al}_2\text{O}_3$ Fe BD). This amount seems to be higher compared to after the first step of modification ( $\text{Al}_2\text{O}_3$  Fe AM) that is a logical conclusion drawn from the molecular mass of two modifiers where BD has a much higher molecule compared to the AM. “The silane attaches to the OH bond on the surface of the material, but BD should be linked only on the site of the silane molecule already present on the particle. From the TG data it was calculated, in the case of  $\text{Al}_2\text{O}_3$  Fe the ratio of the difference in a weight loss of BD- and AM- modified particles and the weight loss of AM modified particles is 31.7% and in the case of  $\text{Al}_2\text{O}_3$  n, it is 42.0%. The data explain that the process is entirely dependent on the esterification reaction and that the surface of the particle itself does not play any role in the modification of the surface. Analysis of DTG peaks indicated that the first peak (25-150 °C) corresponded to the dehydration of water molecules on the surface and the second peak (150-600 °C) was attributed to silane debonding” [85].

The spherical  $\text{Al}_2\text{O}_3$  n nanoparticles having the  $\gamma$  phase crystal structure showed a high-water adsorption. Water absorption capacity of the synthesized  $\text{Al}_2\text{O}_3$  Fe particles was lower and this is because they have smaller number of hydroxyl groups on the surface and

lower specific surface area. Hydroxyl groups on the alumina surface are the way to enable linking with silane coupling agents.

**Table 2 TGA analysis of alumina particles before and after surface modifications**

Sample	Weight loss (%) (25-150 °C)	Weight loss (%) (150-600 °C)	Mass residual (%) (800 °C)	DTG peaks (800 °C)
Al <sub>2</sub> O <sub>3</sub> Fe	3.97	2.59	93.44	45
Al <sub>2</sub> O <sub>3</sub> Fe AM	1.86	6.09	92.05	54/159/407
Al <sub>2</sub> O <sub>3</sub> Fe BD	5.98	8.02	86.00	57/102/421/526
Al <sub>2</sub> O <sub>3</sub> n	5.36	3.50	91.14	47
Al <sub>2</sub> O <sub>3</sub> n AM	2.96	12.98	84.06	58/247/407
Al <sub>2</sub> O <sub>3</sub> n BD	6.32	18.43	75.25	103/244/435

## **5. Composite films using modified and as produced alumina particles as reinforcement and photopolymerized matrix film**

One of the possible uses of modified alumina particles is in composite films deposited on the metal substrate. The metal substrate was chosen as this sort of materials needs protection from environment conditions. Addition of ceramic based particles improves the hardness of the film, and if the particles are surface modified the modification can improve contacts of the film and the substrate.

### **5.1 Composite films preparation**

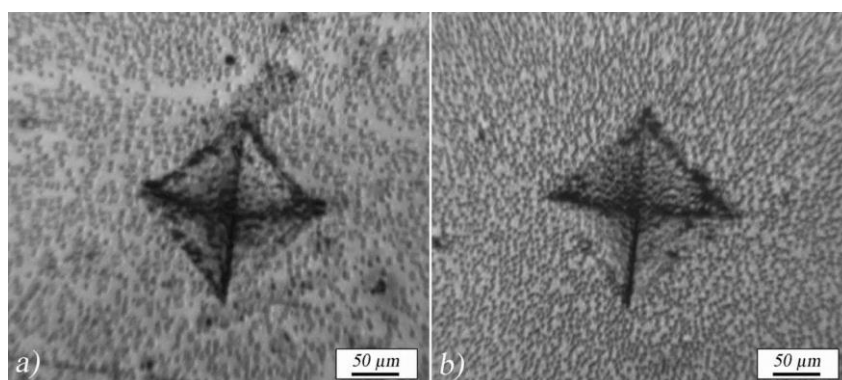
Brass was chosen to be the substrate in this research. The hardness was 260 ½ (ASTM B36 250 µm-thick (ASTM B36, K&S Engineering). Brass consisted of copper 68,5-71,7 mass %, zinc 28-32% and traces of lead and iron less than 0,1 mass %. In order to prepare the surface of the brass it was treated using a 20% sulfuric acid solution [108].

This process is activating the surface, cleans all rests of the possible organic compounds and prepares the surface for deposition of the composite film. The composite film was compared to the pure polymer film that consisted of: Bis-GMA 49.5 %, TEGDMA 49.5 %, CQ 0.2 % and 4EDMAB, 0.8 % and cured under UV light. Composite films contained: 0.5 wt. %, 1.5 wt. % and 3 wt. % of modified alumina particles [109]. Polymer films were

prepared by the drop coating method. Single drop of a composite precursor in liquid form is deposited on the brass surface, then a thin cover is posed over and the monomer is polymerized to the form the composite. The film was then polymerized under UV light for 3 minutes. The weight of the class plate controlled the deposited composite producing the film thickness of  $70 \pm 5 \mu\text{m}$ .

## 5.2 Hardness measurements of composite films – results and discussion

The film hardness is studied as the mechanical property that enables the characterisation of mechanical properties of materials. For films hardness is very important as it is describing the properties of the material and the surface of the film has to resist the scratching. Micro Vickers indentation for composite films prepared with ferrous oxide doped alumina-based particles with AM and BD surface modification of particles are shown in Figure 18. It is clear that the indents are clear and that the surface of the film is uniform.



**Figure 18. Micrograph of micro Vickers indentation for composite films: a) with 0.5 wt. % of  $\text{Al}_2\text{O}_3$  Fe - AM particles, and b) with 0.5 wt. % of  $\text{Al}_2\text{O}_3$  Fe - BD particles [85].**

Plastic deformation resulting from the indentation shown in Figure 18 indicates that there are no changes in the mechanism of plastic deformations in films on the metal substrate. The edge fracture form may indicate the change in composite mechanical properties [110]. The composites have the ability to absorb energy and respond plastically, the surface fracture does not appear at the edge of the produced impression as it can be

seen on micrograph. This behaviour indicates that composites follow the mechanical deformation even as they contain the reinforcement that intend to reduce elasticity/increase brittleness, that results in apparition of multiple cracks especially at the corners of the indent morphology [110].

### 5.3 Hardness measurements for adhesion accesement – results and discussion

“The hardness of the samples was measured at micro Vickers machine with different loads (15, 25, 50, 100, 300 and 500 g) for 25 s, whereby for each loading three indents were performed. Images of indentation marks were made by the optical microscope and were used to obtain the diagonal lengths using the Image Pro Plus program for each indent”.

“The mean diameter of the diagonal's composite hardness is entered as input parameters in the model [111]. In order to fit the composite hardness relation on the depth indentation by the model shown by the equation:

$$\Delta H = \left[ \frac{7 \cdot (m+1) \cdot (H_s - H_f)}{m \cdot b} \right] \cdot \frac{t}{d} \quad (1)$$

where A, B, C are the fitting parameters, H<sub>c</sub> is the composite hardness and m is a parameter called (power index), the values of which are in the range of 1-2 (for soft films on a hard surface m=1.8) [112]. The equation used to calculate the film hardness, is given by”:

$$H_f = A \pm \sqrt{\frac{[m|B|/(m+1)]^{m+1}}{m|C|}} \quad (2)$$

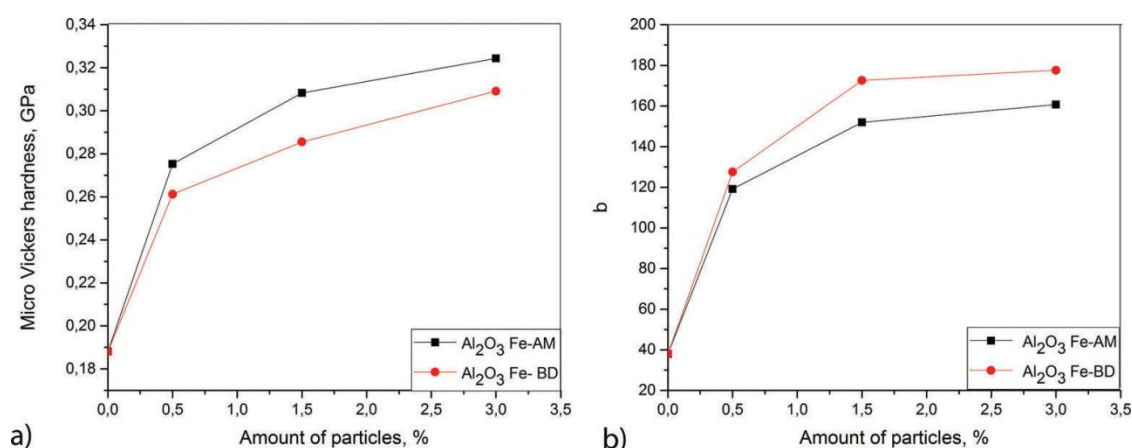
“For the calculation of the critical reduction of depth b the equation (3) is used

$$\Delta H = \left[ \frac{7 \cdot (m+1) \cdot (H_s - H_f)}{m \cdot b} \right] \cdot \frac{t}{d} \quad (3)$$

The depth of the indentation is supposed to be D/7, and t is the film thickness. Values: H<sub>s</sub>, H<sub>c</sub>, and d are obtained by direct experimental measurement, H<sub>f</sub> is determined by fitting the experimental data for H<sub>c</sub> as a function of h / t. Plotting dH = f (t / d) gives the diagram that could be subjected to the linear fit according to the equation (3). The slope of this fit

is the value of parameter  $b$  that could be considered as the measure of adhesion  $b$ . The parameter  $b$ , is the ratio of the radius of the plastic zone under indenter and depth of indentation,  $b = r / h$ , and it changes depending on the combination of the film and the substrate and is the measure of adhesion”.

Figure 19 shows the micro hardness measured on composites with AM and BD modifications of alumina-based particles.



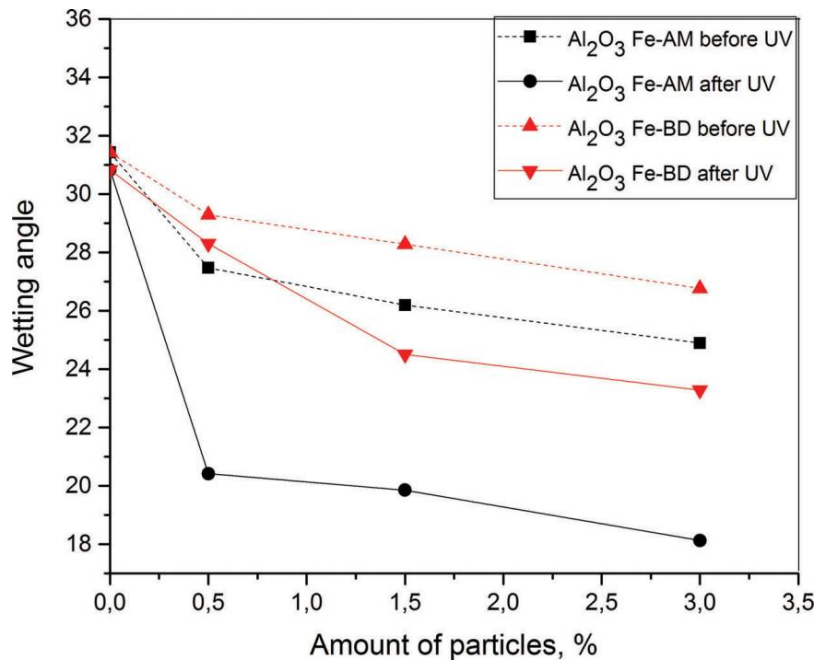
**Figure 19. a) Micro hardness changes regarding the amount of different modifications (AM/BD) of Al<sub>2</sub>O<sub>3</sub> Fe particles, b) the dependence of the adhesion strength parameter  $b$  of the particles share [85].**

Addition of reinforcements modified with AM and BD improve micro hardness of composites with addition of the presented content of fillers. Matrix itself has the micro hardness of 0,1881 GPa. Composites with Al<sub>2</sub>O<sub>3</sub> Fe particles with different modifications (AM/BD) have better hardness, Figure 19. Structure modification with flexible BD of Al<sub>2</sub>O<sub>3</sub> Fe in composite increases hardness when small additions even as low as 0.5 wt. % increase the hardness by 39%, and addition of 3 wt. % of Al<sub>2</sub>O<sub>3</sub> Fe-BD reinforcements improves the hardness by 64%. Adhesion parameter  $b$  was 4 times that of the matrix for the composite having 3 wt. % Al<sub>2</sub>O<sub>3</sub> Fe-AM and more than 3 times improved with Al<sub>2</sub>O<sub>3</sub> Fe-BD particles (323%).

Particles Al<sub>2</sub>O<sub>3</sub> Fe-AM produced increase of hardness, compared to pure matrix, from 46%, for the addition of particles of 0.5 wt. %, to 72% for 3 wt. % of reinforcing particles

addition. The adhesion parameter of composite with 3 wt. % of Al<sub>2</sub>O<sub>3</sub> Fe-AM particles was improved nearly 4 times (367%), compared to the pure resin. Hydrogen bonding with OH groups of Bis-GMA matrix component is improving the reinforcement of composite with Al<sub>2</sub>O<sub>3</sub> Fe-AM particles. Important increase of the adhesion with the substrate is also observed in those composites. BD modification on Al<sub>2</sub>O<sub>3</sub> Fe-BD particles contain the vinyl group modified surface that participates in different intermolecular interactions:  $\pi$ ,  $\pi$ -stacking, dipolar and hydrogen bonding interactions [91]. Spatial conformation of BD leads to the spherical wrapped structure stabilized by hydrogen bonding interactions, representing a slight steric hindrance to double bond availability in cross-linking reaction during composite curing and establishing of hydrogen interactions with the matrix [85]. Flexible aliphatic chains of BD caused a bit lower hardness of composite reinforced with Al<sub>2</sub>O<sub>3</sub> Fe-BD particles compared to that reinforced with Al<sub>2</sub>O<sub>3</sub> Fe-AM. A significant increase in hardness and adhesion parameter for both types of particles indicates that when modified particles are used a very small amount is needed to improve the material properties [85]. Wear resistance is usually proportional to the improved hardness of the material. Also improved hardness is contributing to cutting, and scratching of the coating and improves the possible use of the material in industrial applications.

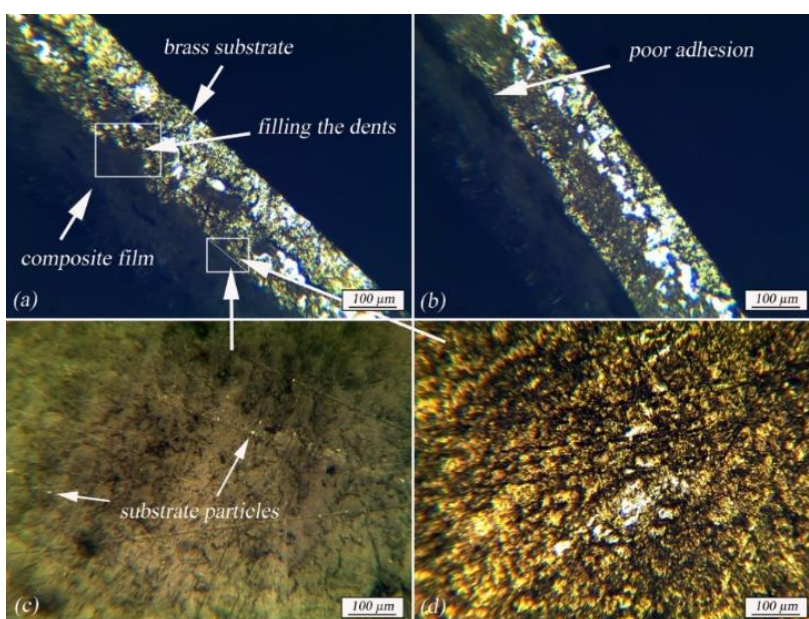
Decrease of wetting angles illustrates better adhesion of the composite to the substrate. Better adhesion is visible in the prepared precursors and it is reflected in the formed composites. This measurement results are shown in Figure 20.



**Figure 20. Dependence of the wetting angle for composite films in the moment of application on the substrate and after UV light exposure [85].**

Importance of the adhesion of the coating is related to the wetting angle of the precursor on the interface [113]. The contact angles of the composite mixture with Al<sub>2</sub>O<sub>3</sub> Fe particles with different modifications decreased with increasing the content of particles in the composite. Once the composite film has properly wetted the substrate surface, the adhesion can be performed through three mechanisms: chemical bonding, mechanical interlocking and diffusion mechanisms [85]. The decrease of contact angle for different composite films is obvious in Figure 20. The measured contact angles are presented in the function of particle content in the composite. Low contact angle enables good wetting and then the adhesive flows into the valleys and crevices on the metal surface which may be noticed on the composite film/substrate cross-section, Figure 21. Higher contact angle results in poor wetting when the adhesive bridges over the valleys and results in a reduction of the actual contact area between the adhesive and the adhered, resulting in a lower overall joint strength, Figure 21 [114]. The surface roughness of brass substrate from Figure 21 is mostly of interest for mechanical interlocking, since it is ranging in a scale of hundreds of nanometres to few microns with a film thickness of 0.1–100 μm

[113]. Adhesion reached at the interface can also be improved by the use of organosilanes as adhesive primers by the hydrolytic reaction of silanols and hydroxyl functions from the metal surface (chemical bonding). Organosilane modifications at the alumina surface in the composite film influences the adhesive strength resulting in increase of adhesion parameter  $b$  compared to the composite film reinforced with neat  $\text{Al}_2\text{O}_3$  Fe particles (17.2%) [115]. An overall increase in adhesion strength can be seen by the drawn-out particles of the substrate on the adhered surface of the separated composite film, Figure 21c. Figure 21c and d represent the inner surface of composite film and metal substrate, respectively, with a closely matching microstructure indicating that the low wetting angle (surface tension) enabled good wetting of the substrate, which was the first and essential requirement in establishing good adhesion [85].



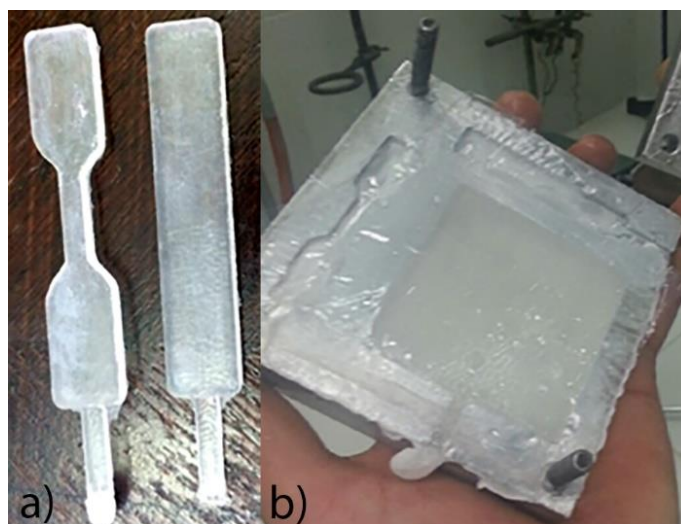
**Figure 21. (I) Cross-section of the adhered composite films with (a)  $\text{Al}_2\text{O}_3$  Fe-AM particles, and (b)  $\text{Al}_2\text{O}_3$  Fe-BD particles, (II) contact surface of the (c) composite film and (d) substrate – brass [85].**



## 6 Composite materials having alumina particles, modified alumina particles and PMMA-itaconate matrix

### 6.1 Preparation of PMMA/DMI composites reinforced with alumina particles

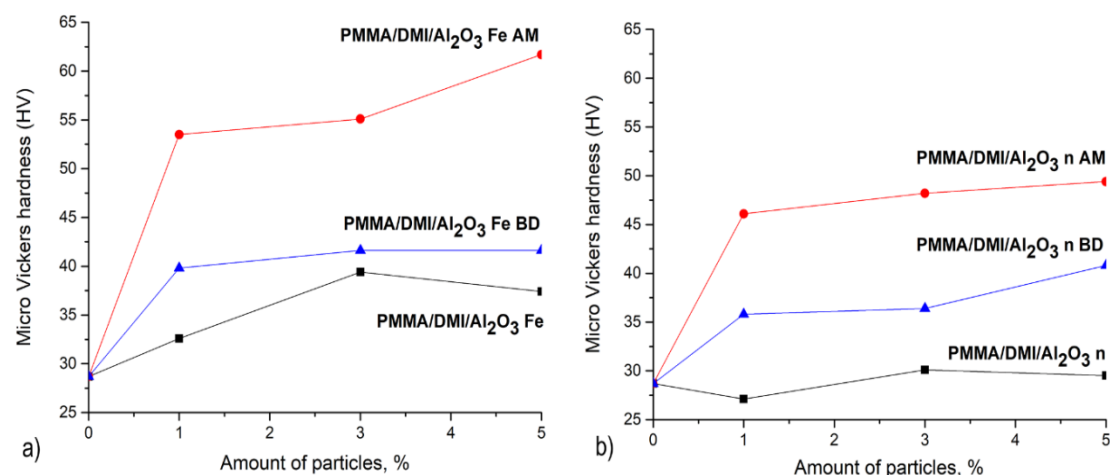
“The matrix consisted of PMMA and DMI that presented the 5 wt. % of DMI. DMI was added to the PMMA monomer and the liquid was added to the prepolymerized powder of PMMA. Particles were added to the liquid and the mixture was dispersed in an ultrasound bath for 30 minutes to avoid agglomeration and achieve good dispersion. The powder component (63 wt. %) was added to the liquid and stirred for 5 minutes after it was converted into a paste that was placed in a mold made of an aluminum alloy. The mold was closed and heated to 70 °C for 1 h, after which polymerization was completed at 100 °C in 30 minutes. The samples were prepared using 1 wt. %, 3 wt. % and 5 wt. % of different alumina particles (ferrous oxide doped alumina particles and alumina nanoparticles with two surface modifications). The polymer matrix consisting of PMMA and DMI is designated as PMMA/DMI (hereafter DMI)” [85].



**Figure 22. a) The specimens for tensile testing b) The mold for sample preparation showing the forms for preparation of the sample for tensile testing and for high speed impact testing.**

## 6.2 Microhardness of composite materials – results and discussion

“Micro Vickers hardness (HV) method was used to measure hardness of the PMMA/DMI composites. The results are presented in Figure 23. The microhardness values are compared with those of composites in which the alumina particles were not modified” [109].



**Figure 23. “Micro Vickers hardness of PMMA/DMI matrix and composites reinforced with a) ferrous oxide doped alumina-based particles and b) alumina nanoparticles” [87].**

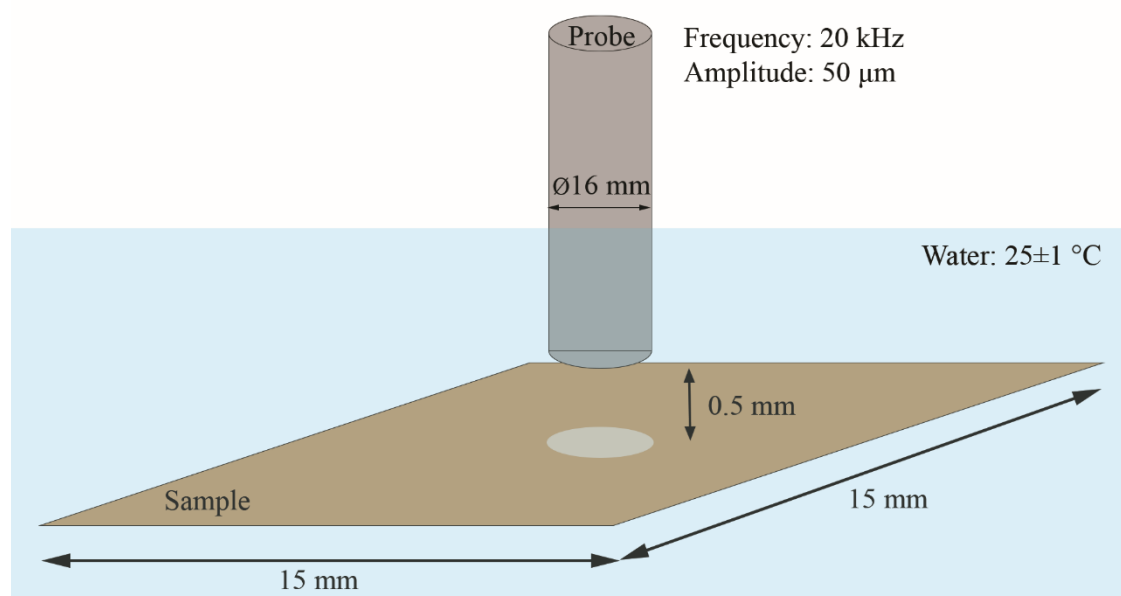
“The best hardness values were observed in composite consisting of the matrix reinforced with ferrous oxide doped alumina particles and AM surface modification (Al<sub>2</sub>O<sub>3</sub> Fe AM)” [87]. Hardness increased for further addition of particles being the higher in composites having 3% and 5% of reinforcement. The composites with Al<sub>2</sub>O<sub>3</sub> Fe AM particles had a hardness of 46.4% to 53.5%, compared to the PMMA/DMI matrix. BD surface modification of ferrous oxide doped alumina particles formed composites having increased hardness by 27.9% to “31.1% relative to the matrix. Alumina nanoparticles with surface modification (Al<sub>2</sub>O<sub>3</sub> n AM), gave the composite hardness increase by 37,7% to 41.9%. The hardness of composites with surface-modified particles in relation to unmodified particles was important” [87]. Unmodified ferrous oxide doped alumina particles in PMMA/DMI matrix increased the hardness by 27,2% compared to polymer

blend of (PMMA/DMI) having no reinforcements, whereas unmodified alumina nanoparticles increased the hardness by 4,6%.

“The composite reinforced using  $\text{Al}_2\text{O}_3$  Fe particles without modification has hardness higher of that reinforced using  $\text{Al}_2\text{O}_3$  n. Commercial alumina particles,  $\text{Al}_2\text{O}_3$  n were mostly  $\gamma$ -alumina their improvement in hardness is less important compared to particles that have more  $\alpha$  alumina in their crystal structure. Corundum or  $\alpha$  alumina is the most stable and the hardest of the alumina structures and it influences the hardness of the composite in the same way” [99]. Addition of the surface modification to those particles increases the hardness of the composite but the influence of the crystal structure can be also observed.

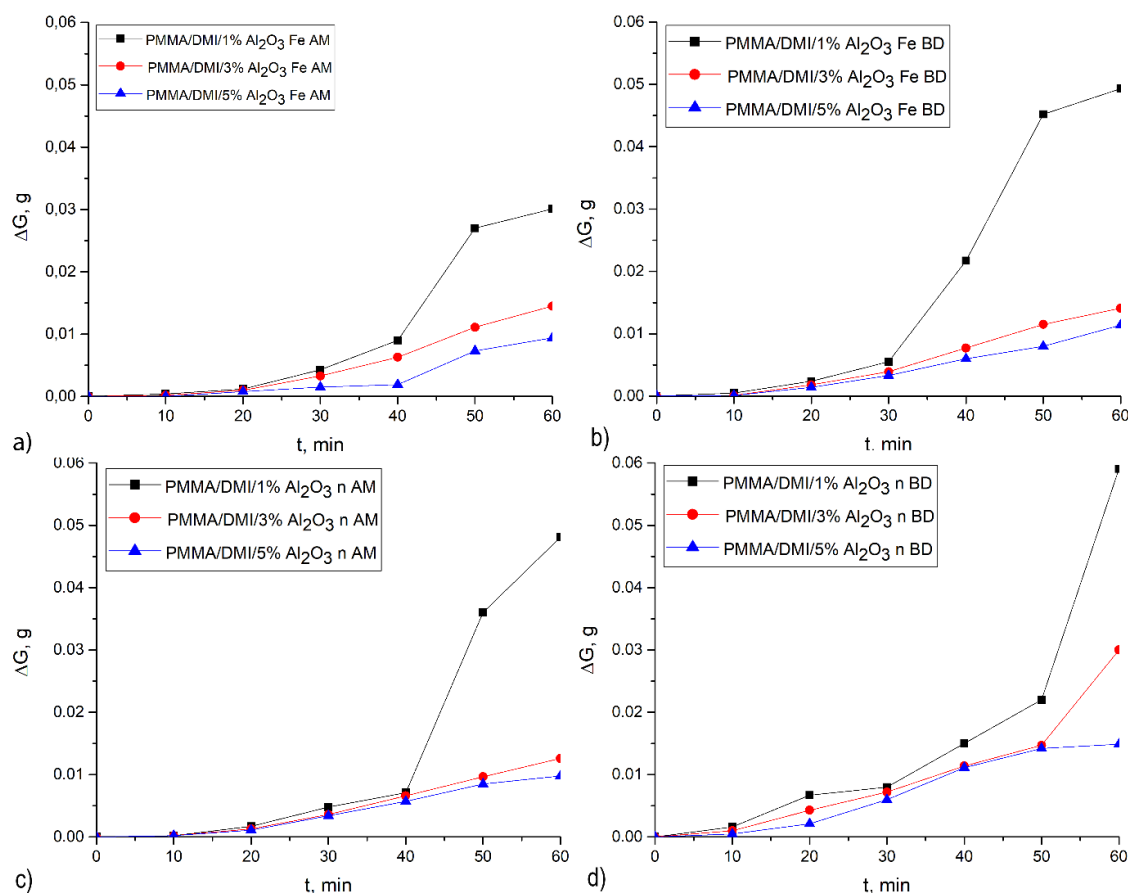
### 6.3 Testing of cavitation erosion - results and discussion

Cavitation is examined using the standard method where the specimen is immersed in water and the cavitation is applied to the surface of the specimen. This is the standard procedure and the specimens are at the same time exposed to cavitation and the water is absorbed by the specimen.



**Figure 24. The experimental setup of the cavitation testing in the stationary fluid [116].**

The cavitation was done in several steps in order to be able to follow the mass loss of the specimen. “The composites exposed to cavitation were dried after each step of exposure at 100 °C for 1 hour and measured using an analytical balance with  $\pm 0.1$  mg accuracy”[109, 115]. The mass loss of composites having reinforcements having surface modifications using the AM and BD is shown in Figure 25.



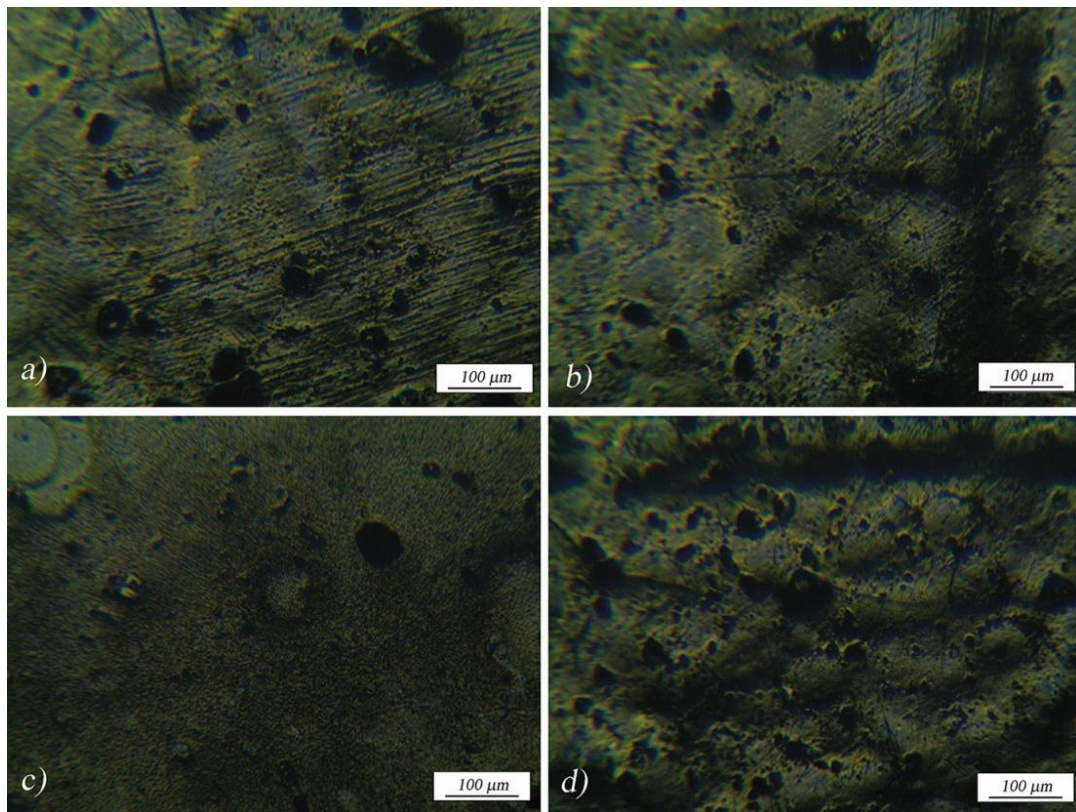
**Figure 25. “Mass loss during cavitation resistance testing of composites with different alumina-based particles: a) PMMA/DMI/Al<sub>2</sub>O<sub>3</sub> Fe AM, b) PMMA/DMI/Al<sub>2</sub>O<sub>3</sub> Fe BD, c) PMMA/DMI/Al<sub>2</sub>O<sub>3</sub> n AM and d) PMMA/DMI/Al<sub>2</sub>O<sub>3</sub> n BD” [87].**

“Ferrous oxide doped alumina-based particles and AM surface modification exhibited the best cavitation resistance” [87]. Figure 25a. The addition of 3% and 5 wt.% improves the cavitation resistance of the composite material. “The trend in the mass loss of samples illustrates the effect of the reinforcement filler in the structure on the mass loss rate of the material. Small quantity of reinforcement, such as 1 wt. %, entered the second cavitation

phase during the first hour of the experiment, whereas a larger amount of the reinforcement produced a material that performed better under harsh experimental conditions, resulting in a material with superior surface resistance” [87].

#### **6.4 Image analysis used to characterize the surface degradation under cavitation of composite**

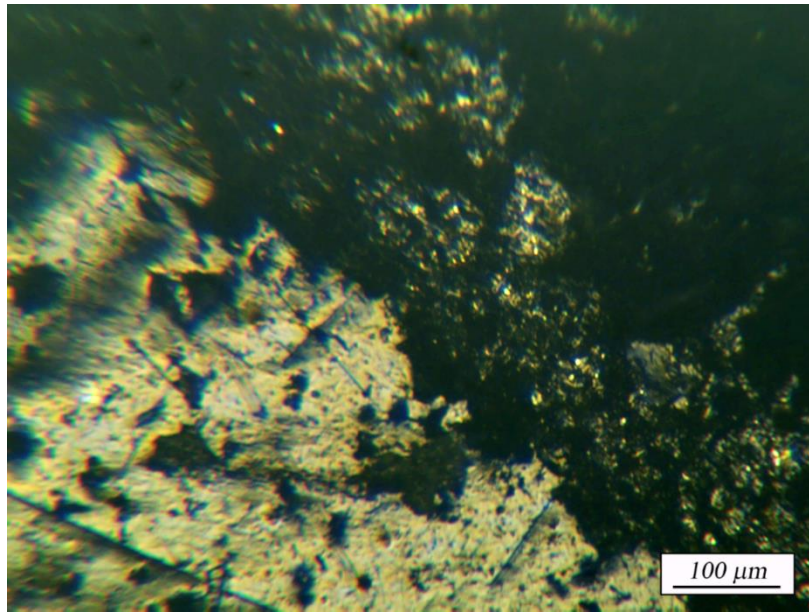
“The control procedure that follows the cavitation testing consists of taking an optical micrograph of the specimen with a 600 dpi scanner enabling the resolution that visualizes the defects of 42  $\mu\text{m}$ . Those images revealed that the surface of all specimens is smooth and that the initial conditions on every specimen were the same from the point of view of surface roughness. As the procedure includes the observation of the same specimen those visualizations were done after every specimen mass measurement and enables the following of the surface destruction. The observation of every one of the specimens under SEM would change the surface characteristics as it would change the surface with the preparation with the layer of gold that enables the observation but also some changes could occur due to the influence of the electron beam. So, the decision was made to observe the specimens having the lowest destruction under the SEM and AFM once the cavitation testing ended. Those analyses were done in order to have the information about the quality of the surface after exposition to cavitation. The specimens having 5 wt. % of the reinforcement was further analyzed. The surfaces of the best performing specimens before exposition to cavitation were observed under the optical microscope and their images are given in Figure 26. It could be seen that all four specimens are having similar surface quality. In Figure 27, the region that represents the region that was exposed to cavitation and the nearby region that was not damaged are photographed under an optical microscope. It is clear that one can easily spot the difference but optical micrographs do not enable any measurements to be done of the details on the surface. In order to analyze the surface quality after 60 min of exposition to cavitation, the surface was observed under the FE-SEM” [87].



**Figure 26. “Optical micrographs of surfaces of specimens prior to cavitation exposure having 5 wt. % of particles reinforced using the a)  $\text{Al}_2\text{O}_3$  Fe AM, b)  $\text{Al}_2\text{O}_3$  Fe BD, c)  $\text{Al}_2\text{O}_3$  n AM and d)  $\text{Al}_2\text{O}_3$  n BD” [87].**

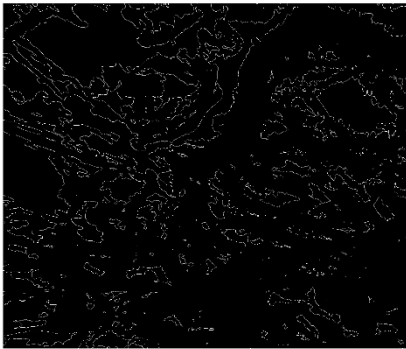
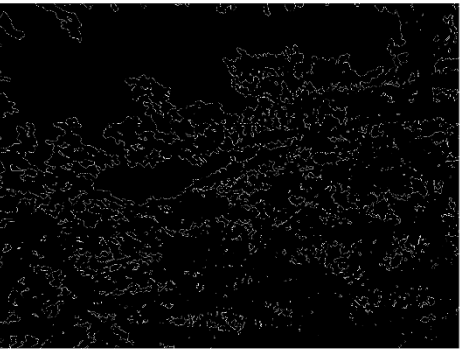

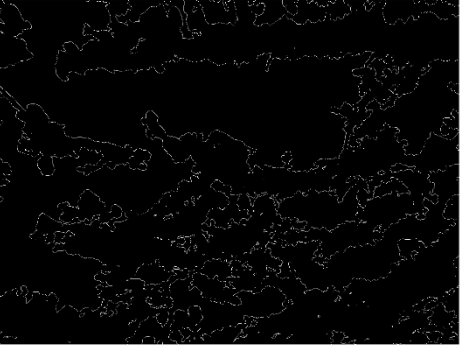


Initial structures surfaces of fresh specimens were analyzed using the image analysis. All the specimens were prepared using the same procedure in the same mold resulting in a very similar surface. The images were taken using the optical microscope and are presented together. For the purpose of comparing the surface texture of specimens the digital images were processed using the algorithm to obtain the Hausdorff dimension that describes the quality of the features on the surface. The values of the obtained Hausdorff dimension differed only slightly from image to image and it could be concluded that the surface was similar enough on all specimens at the beginning of the test. Results of those analyses are presented in Table 3.





**Figure 27. “The region on the surface of the specimen having 5 wt. % of alumina modified using AM reinforcement showing the obvious difference between the region subjected to cavitation and the region that was out of the reach of the jet” [87].**

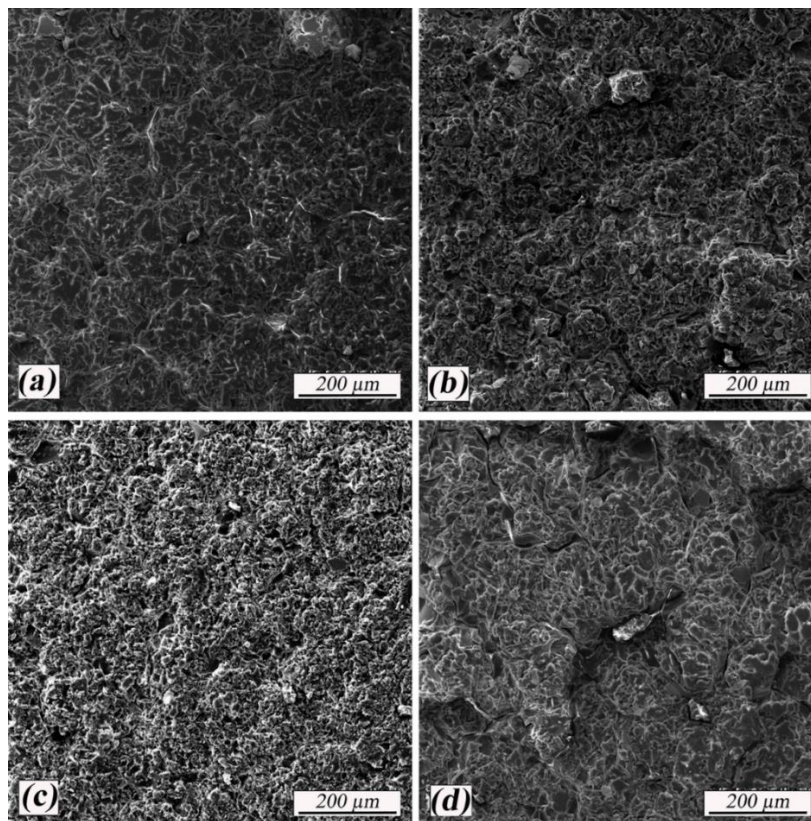
**Table 3 Hausdorff dimension analysis of initial structures of composites having AM and BD modifications illustrating that the initial structure was mostly influenced by the way of preparation and that the resulting characterisation gave similar quantitative measurement**

	Al AM	Al BD
1 wt.%	Hausdorff Dimension = 1.933 	Hausdorff Dimension = 1.934 
3 wt.%	Hausdorff Dimension = 1.854 	Hausdorff Dimension = 1.886 
5 wt.%	Hausdorff Dimension = 1.763 	Hausdorff Dimension = 1.821 



As cavitation, as a very destructive process, destroys the surface of the specimen it became dark and impossible to observe features using the optical microscope. So it was decided to test the best performing specimens using the SEM in order to be able to observe the quality of the surface obtained. The region where the cavitation influence stops and the joint of two regions it is obvious that the optical microscopy is not appropriate to characterize those specimens.

“The FE-SEM micrographs showing surface defects after 60 minutes of cavitation for composite with 5 wt. % of AM and BS modified alumina particles and two surface modifications are presented in Figure 28” [87].

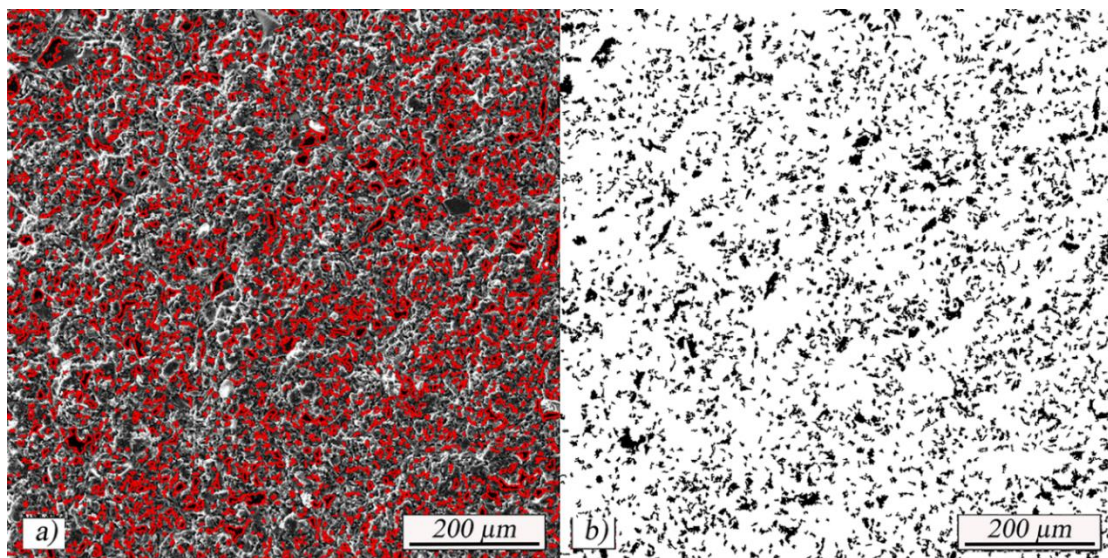


**Figure 28. “FE-SEM micrographs of surface morphology of composites after cavitation in PMMA/DMI matrix with 5 wt. % of: a)  $\text{Al}_2\text{O}_3$  Fe AM, b)  $\text{Al}_2\text{O}_3$  Fe BD, c)  $\text{Al}_2\text{O}_3$  n AM and d)  $\text{Al}_2\text{O}_3$  n BD” [87].**

The FE-SEM image of the surface of the eroded specimen analyzed by image analysis. As the image was taken on the surface that was not perfect due to previous explosion to

cavitation adaptive thresholding procedure was needed for selection of objects having defined characteristics. Several images of every specimen were taken and subjected to the same procedure. “Morphological characteristics of observed defects were compared with the aim to obtain as detailed information as possible about the influence of the cavitation jet on the surface” [117].

Figure 29 “illustrates how surface damage of the sample exposed to cavitation was determined” [87].



**Figure 29. “a) Extraction of defects by adaptive threshold defects selection and b) binary image mask used for surface defect characterization” [87].**

“The values of the surface damage of the samples from 5 wt. % of different alumina particles and two surface modifications exposed to cavitation after 60 minutes are shown in Table 3” [87].

**Table 4 “Comparison of hardness and surface damage parameters of samples exposed to cavitation after 60 minutes (samples with 5 wt. % of different alumina particles and two surface modifications)” [87].**

<b>Samples</b>	<b>Micro Vickers hardness</b>	<b>Defects/mm<sup>2</sup></b>	<b><i>D</i><sub>mean</sub> μm</b>
PMMA/DMI/Al <sub>2</sub> O <sub>3</sub> Fe AM	61.7	496	10.6
PMMA/DMI/Al <sub>2</sub> O <sub>3</sub> Fe BD	41.6	1005	24.9
PMMA/DMI/Al <sub>2</sub> O <sub>3</sub> n AM	49.5	844	11.8
PMMA/DMI/Al <sub>2</sub> O <sub>3</sub> n BD	40.8	1088	26.5

“Surface damage was characterized here as the part of the surface where the deepest defects arise and this corresponded to the formation of pits, inherent to cavitation” [87]. Damage develops around the formed pits. “In this analysis, the amount of those deepest defects on the surface was calculated. The number of defects was normalized per mm<sup>2</sup> in order to enable comparison among samples” [87]. The number of defects in samples modified using the AM was lower and defects were smaller in size. “Particle surface modification using the BD modification enables the stabilization of the bond and it should be beneficial for the specimens serving in water” [87]. BD surface modified particles used as reinforcement didn’t have the appropriate resistance to cavitation and the surface had larger number and generally bigger size of surface defects per unit of the surface measured.

Hardness and cavitation resistance both characterize the surface of a material. This trend was observed on metallic specimens [118]. The values of hardness were compared to the number of surface defects observed on specimens. The good correlation between those two characteristics was observed. “The best hardness values correspond to the lowest number of surface damage points. The hardness measurement can indicate the possibility to improve the resistance of the surface of the composite” [118].

AFM was performed with NanoScope 3D (Veeco, USA) microscope operated in tapping mode under ambient conditions. Etched silicon probes with spring constant 20 – 80 Nm-

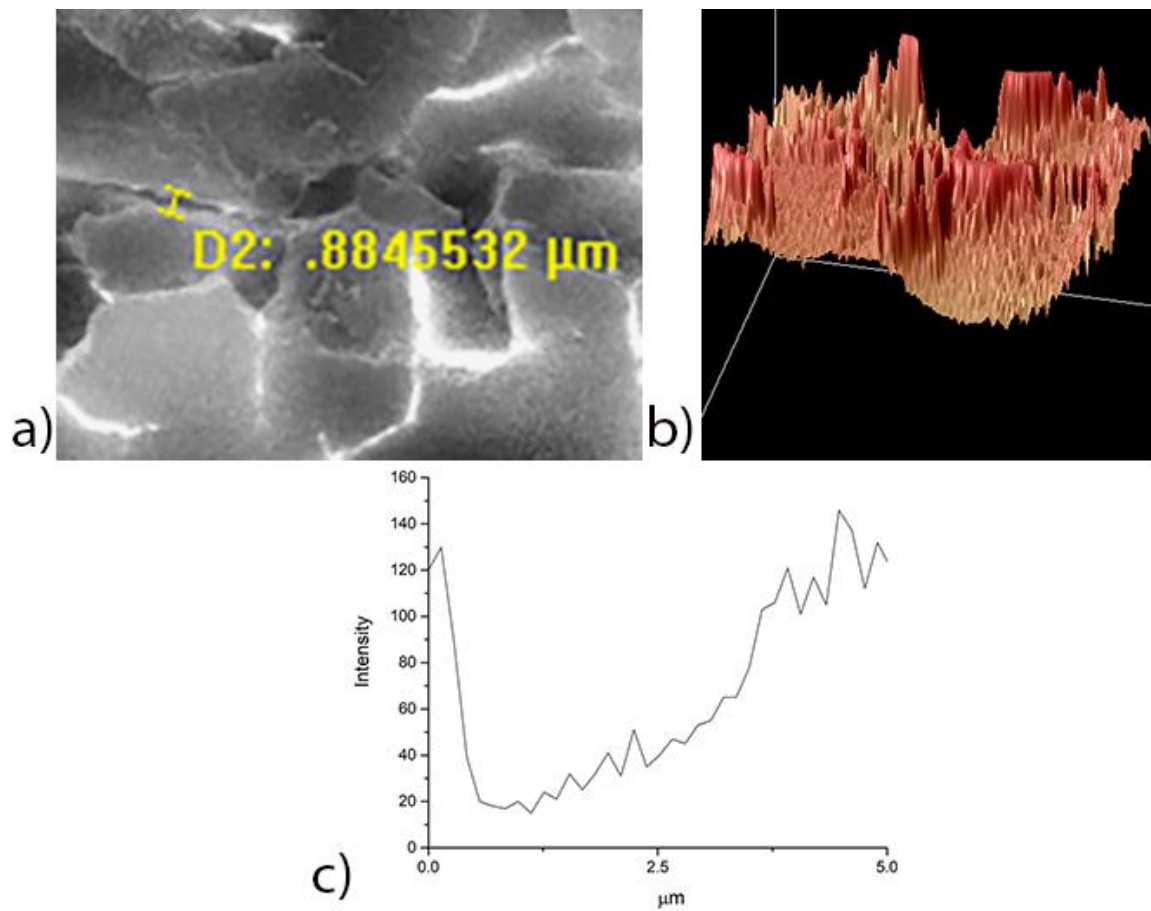
1 were used. The surface roughness (RMS) is calculated as the root mean square average of height deviation:

$$\sqrt{\frac{\sum Z_i^2}{n}} = RMS$$

Where  $Z_i$  is the maximum vertical distance between the highest and lowest data points in the image,  $n$  is a number of measurements.

### **6.5. AFM analysis of the composite specimen surface after surface erosion**

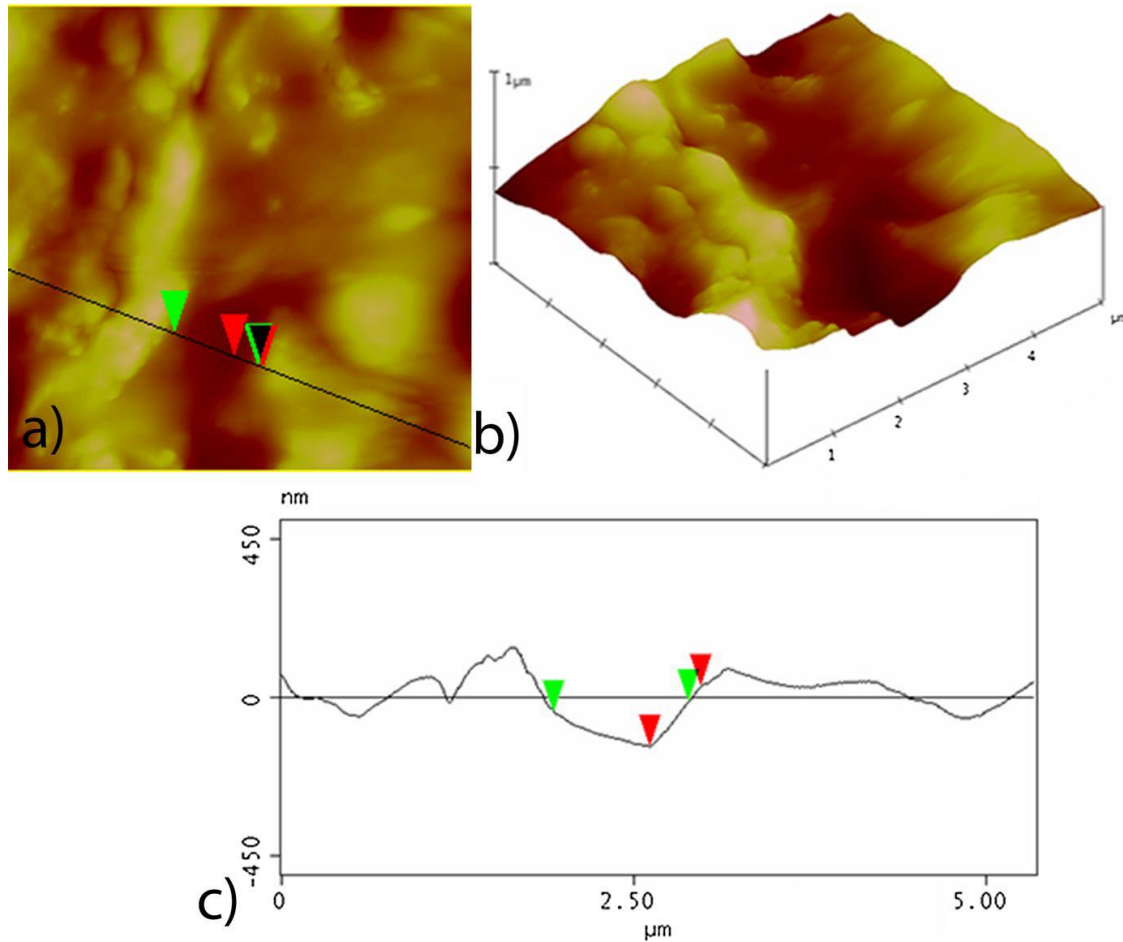
“For the best performing sample, the one reinforced with  $Al_2O_3$  Fe AM, the higher resolution SEM and the sample was observed under the AFM. The image is presented in Figure 30. The same sample was observed using the AFM microscope and the results of observed surface features are compared in Figure 31. The used AFM has very high resolution and the part of the damaged surface analyzed is very small. The observed width of the damage is given in the image Figure 31c” [87].



**Figure 30. “SEM Section Analysis of composite with  $\text{Al}_2\text{O}_3$  Fe AM, ( $21\mu\text{m} \times 16 \mu\text{m}$ ): a) View of the analyzed surface, b) surface plot of the observed surface, c) line profile analysis” [87].**

“The distance of the weight of damage is 884.55 nm and the height of the surface damage is marked on the image is about 130 nm of arbitrary units” [87].





**Figure 31. AFM Section Analysis of composite with Al<sub>2</sub>O<sub>3</sub> Fe AM, (5 μm x 5 μm x 1 μm): a) View of the analyzed surface, b) surface plot of the observed surface, c) line profile analysis [87].**

The distance between green markers that are at the same level of the observed specimen is 957.03 nm and the distance from the lowest to the highest part of the damage is marked on the image is 171.62 nm.

All the information obtained from the AFM is very detailed and enables obtaining the exact data about the depth of the surface damage caused by cavitation. The main disadvantage of this study method is that it is time-consuming and the experimental cost is very elevated. The information is therefore compared to that obtained from the SEM

image that enables the observation of a larger surface. The disadvantage of the SEM image is that it offers the possibility to measure surface distances among features observed in the image, but the depth of the damage should be estimated from the darkness observed. Once the comparison of two methods is given it could be concluded that the data about the distances among damages observed, their form and frequency of apparition could be compared without any hesitation. The only reserve about the SEM image remains about the depth interpretation. The importance of data collected from the SEM image could be regarded using the information from a much larger surface to obtain more general information. The other remaining problem for the SEM image dealing with the conditions of information collection regarding the position of the studied part from the image could be solved by using only the center part of the SEM image where the conditions are similar enabling the information-driven from this analysis is consistent [87].

## **6.6 Toughness of specimens measured by controlled energy impact testing**

Usually the material design is guided by needs of the user that are much influencing the choice of the research direction. Usually the addition of the reinforcements into the matrix leads to improvement in the material hardness, modulus and strength but sometimes the toughness of the material is hard to improve and to be at the same level with other mechanical characteristics of the material. This feature can be tested using some standard equipment but the controlled energy impact testing is the method that enables the control of several parameters and is adjustable to the material class so the results are good comparison of behavior of series of composites produced. In this research two different surface modifications resulted in different materials having improved surface characteristics, and also having better cavitation resistance but the performance of the material needs to replay to demands in toughness.

“The resistance of composite materials to high-speed impact was assessed on a High-Speed Puncture Impact testing machine HYDROSHOT HITS-P10, Shimadzu, Japan, Figure 32. The composites reinforced with commercial alumina nanoparticles, synthesized ferrous oxide doped alumina particles, with AM, and BD surface

modifications, were tested. The results provided information about the behavior of the composite in a sudden impact situation (Figure 32)” [87].



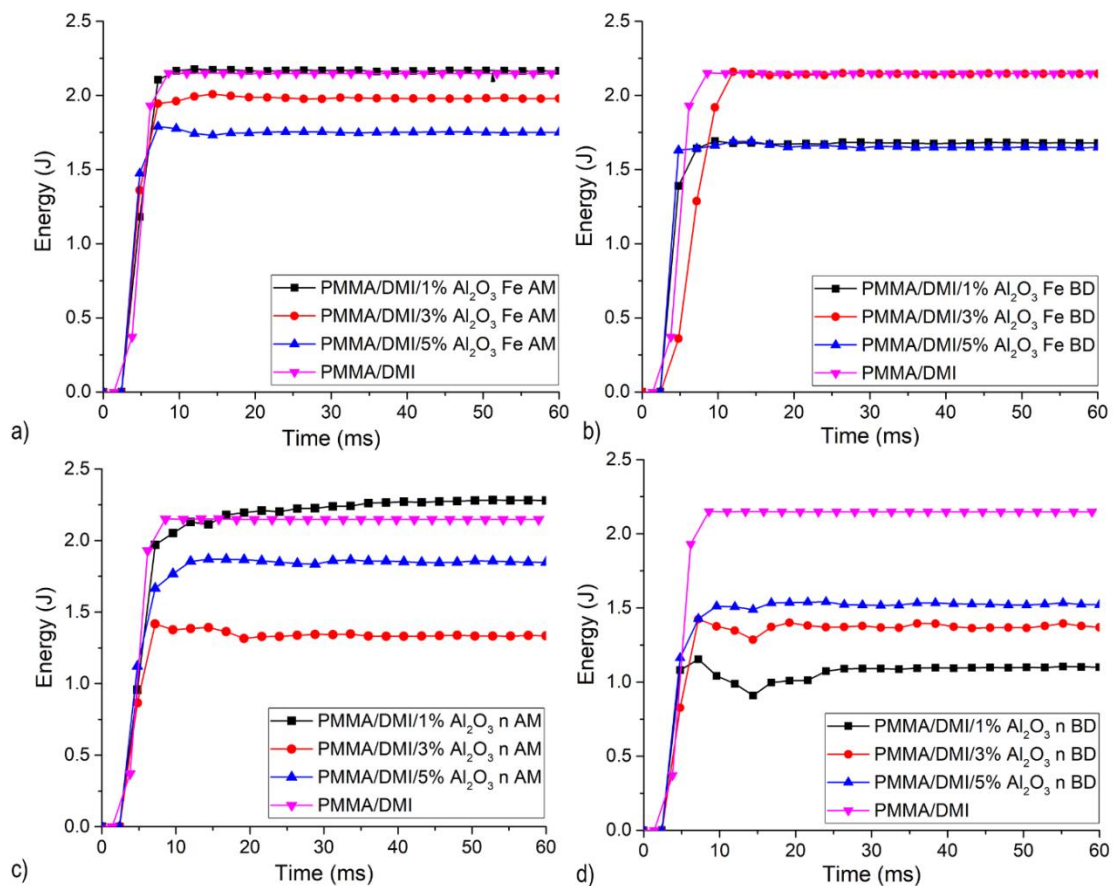
**Figure 32. “Specimen for high-speed impact testing in the testing machine after impact” [87].**

“It is apparent that the composite doped with 1 wt. % particles and AM surface modification of the particles demonstrated the best impact performance, as shown in Figure 33. The specimens exhibited a typical brittle fracture in all impact experiments, except for the composite reinforced with a 1 wt. % of  $\text{Al}_2\text{O}_3$  Fe AM and  $\text{Al}_2\text{O}_3$  n AM, which showed ductile failure. The worst impact performer was the composite doped with alumina nanoparticles and BD surface modification” [87].

“It is observed that the addition of 1 wt. % of particles does not change the substantially the toughness of the material. In the case of the  $\text{Al}_2\text{O}_3$  n particles, it even improves the toughness of the material. Addition of 3 wt.% and 5 wt.% of particles lowers toughness of the specimen and the obtained specimens are less tough. The loss of toughness can be explained by the observation of the particles that create strong bonds with the matrix resulting in higher hardness and modulus” [87]. “The addition of the second layer BD on the initial layer in both sorts of particles is decreasing the toughness. This phenomenon could be also explained by the addition of the layer that does not create springs in the



bonding of particles to the matrix but rather it creates very strong bonds that include several primary bonds between the added molecule and the matrix and therefore the material performs worth when exposed to the impact test” [87]. “The loss of toughness could be accepted as the performance of the material in cavitation and surface destruction is better. On the other hand, the bonds that include the second layer are stabilizing the Al-O-Si bond that could be subject to hydrolysis if the material is immersed in water” [85].



**Figure 33. “Energy–time curves obtained from impact tests of samples with alumina-based reinforcement: a) PMMA/DMI/Al<sub>2</sub>O<sub>3</sub> Fe AM, b) PMMA/DMI/Al<sub>2</sub>O<sub>3</sub> Fe BD, c) PMMA/DMI/Al<sub>2</sub>O<sub>3</sub> n AM and d) PMMA/DMI/Al<sub>2</sub>O<sub>3</sub> n BD” [87].**

## 7. CONCLUSION

The ferrous oxide doped alumina-based particles with different surface modifications of particles (AM/BD) were used as reinforcement in the matrix based on Bis-GMA/TEGDMA. The FTIR analysis proved the effective surface modification of each particle specimen and improved hydrolysis resistance of Al<sub>2</sub>O<sub>3</sub> Fe-BD particles. Wetting angle determination showed increased hydrophobicity but still hydrophilic Al<sub>2</sub>O<sub>3</sub> Fe-AM particles and hydrophobic nature of Al<sub>2</sub>O<sub>3</sub> Fe-BD. Addition of the 3 wt.% of modified Al<sub>2</sub>O<sub>3</sub> Fe-BD and Al<sub>2</sub>O<sub>3</sub> Fe-AM particles caused an improvement of the film hardness, 64%, and 72%, while adhesion parameter *b* increases nearly by 4.2 (323%) for AM modification and 4.7 times (367%) for BD modification. The improvement of adhesion for both films was confirmed by the observation and measurements of the contact angle. The contact angle was measured at the moment when the drop was positioned on the surface and after UV curing and those results proved improved compatibility to the surface compared to pure polymer. A modification of alumina particles by aliphatic olefin (linseed oil esters – BD) enabled the protection and stabilization of the Al-O-Si bond and additionally improves the adhesion and mechanical properties of composite films [85].

“Alumina particles with an enriched alpha crystal phase structure (Al<sub>2</sub>O<sub>3</sub> Fe) improved the hardness of the composites by up to 99%, compared to a pure PMMA matrix [63]. Toughness measured using the high-speed impact test showed that the alumina particles with a large specific surface area (particles with crystal structure rich in transition phases) increased the toughness of the composites”[88, 119]. “Surface modification of alumina particles doped with iron oxide significantly increased the cavitation resistance of acrylate composite films” [120]. “The interphase between the reinforcement and the matrix affects the performance of a composite. This bond is made stronger due to modifying the surface of the reinforcement by different methods. Ferrous oxide doped alumina particles were chosen as a promising type to be modified. In order to compare the effect of modification on the mechanical properties, pure alumina particles having a  $\gamma$  alumina structure were selected to establish a correlation between the surface and crystal structure modifications and the mechanical properties of the composite” [95]. “Two different modifications were

used to compare the behavior of the composite's modifier with a simple silane structure to the modification composed of a long molecule added to the bonds that enable modification of the mechanical properties of the composite" [88]. The results and measurements presented in this study served to determine the effect of the type of modifier deposit on the particle surface, with regard to both mechanical properties and cavitation resistance.

"Composites that have PMMA as the base matrix polymer was prepared by adding DMI and using modified alumina-based particles as reinforcement. Two types of surface-modified (AM/BD) particles were used as reinforcement of the composite materials. The particles with AM surface modification exhibited higher hardness values (41.9% to 53.5%) than those with BD surface modification. Hardness increased with increasing amounts of particles. Hardness was also greater than that of composites prepared with unmodified particles. The hardness values and the extent of surface damage to the samples exposed to cavitation were compared. The highest hardness values corresponded to the smallest surface damage. The various particles and surface modifications of the particles had a different effect on the resistance of the composites to cavitation. The composite with ferrous oxide doped alumina particles and AM particle surface modification exhibited the best cavitation resistance in terms of mass loss and surface degradation level. The worst was a surface modification of alumina particles with BD. A high-speed impact test was used to compare the behavior of synthesized composite materials, with different alumina fillers and with two surface modification, in a high impact situation. The addition of synthesized ferrous oxide doped alumina particles additionally improved impact resistance, compared to commercial nanoparticles. The use of ferrous doped alumina particles, along with AM surface modification, resulted in the best performance during impact testing. The specimen with 1 wt. % of  $\text{Al}_2\text{O}_3$  Fe AM in the PMMA/DMI matrix was demonstrated as a functional dental composite material. The purpose of introducing BD modification of the reinforcement surface was to improve the bond stability established between the silane molecule and the aluminum atom, given that the surface was sensitive to hydrolysis. The modification improved that stability, enhanced some of

the mechanical properties of the material, and enabled the optimization of material properties from a list of requirements” [87].

## 8. REFERENCES

- [1] “<https://offertaformativa.unitn.it/en/lm/materials-and-production-engineering>.” .
- [2] “[https://en.wikipedia.org/wiki/Production\\_engineering](https://en.wikipedia.org/wiki/Production_engineering).” .
- [3] M. Tomii, “A new approach to prehistoric family systems from the viewpoint of pottery usage: Expanding the potential of archaeological information through contextual analysis,” *Quat. Int.*, vol. 474, pp. 182–193, 2018.
- [4] C. Ramesh, N. J. Kumar, and A. K. Malaga, “Fabrication and Mechanical Properties of Iron Slag Matrix Composite Materials,” *Int. J. Eng. Res. Dev.*, vol. 5, pp. 34–46, 2012.
- [5] W. D. Callister, *Fundamentals of materials science and engineering*, vol. 471660817. Wiley London, 2000.
- [6] A. B. Strong, *Fundamentals of composites manufacturing: materials, methods and applications*. Society of Manufacturing Engineers, 2008.
- [7] L. Markovičová, V. Zatkal, V. Šíková, and T. Garbacz, “Effect of UV radiation to change the properties of the composite PA+ GF,” *World Acad. Sci. Eng. Technol. Int. J. Chem. Mol. Nucl. Mater. Metall. Eng.*, vol. 9, no. 10, pp. 1224–1227, 2015.
- [8] A. K. Bledzki and J. Gassan, “Composites reinforced with cellulose based fibres,” *Prog. Polym. Sci.*, vol. 24, no. 2, pp. 221–274, 1999.
- [9] A. K. Mohanty, M. Misra, and L. T. Drzal, “Surface modifications of natural fibers and performance of the resulting biocomposites: an overview,” *Compos. interfaces*, vol. 8, no. 5, pp. 313–343, 2001.
- [10] V. Anandbabu, P. Sathishkumar, B. Sathishkumar, U. Seeman, and G. Surya, “Fabrication and Testing of AL6063/B4C/Gr Hybrid Metal Matrix Composites,” *Int. J. Innov. Res. Sci. Eng. Technol.*, vol. 6, no. 3.
- [11] “The Encyclopedia of Wood Skyhorse Publishing Inc,” 2007.
- [12] A. K. Mohanty, M. Misra, and L. T. Drzal, “Sustainable bio-composites from renewable resources: opportunities and challenges in the green materials world,” *J. Polym. Environ.*, vol. 10, no. 1–2, pp. 19–26, 2002.
- [13] A. K. Bledzki, V. E. Sperber, and O. Faruk, *Natural and wood fibre reinforcement in polymers*, vol. Report No1. iSmithers Rapra Publishing, 2002.

- [14] W. J. Evans, D. H. Isaac, B. C. Suddell, and A. Crosky, "Natural fibres and their composites: A global perspective," in *Proceedings of the... Risø International Symposium on Materials Science*, 2002, pp. 1–14.
- [15] H. B. Vinay, H. K. Govindaraju, and P. Banakar, "A Review on Investigation on the Influence of Reinforcement on Mechanical Properties of Hybrid Composites Introduction," *Int. J. Pure Appl. Sci. Technol. Int. J. Pure Appl. Sci. Technol.*, vol. 24, no. 2, pp. 39–48, 2014.
- [16] M. B. Manju, S. Vignesh, K. S. Nikhil, A. P. Sharaj, and M. Murthy, "Electrical Conductivity Studies of Glass Fiber Reinforced Polymer Composites," *Mater. Today Proc.*, vol. 5, no. 1, pp. 3229–3236, 2018.
- [17] A. K. Senapati, S. Choudhury, S. S. Mishra, R. Roushan, and S. Nanda, "Mechanical and Tribological Analysis of Polymer Matrix Composites," *Int. J. Eng. Adv. Technol.*, vol. 6, no. 4, pp. 193–203, 2017.
- [18] N. Chawla and K. K. Chawla, "Metal-matrix composites in ground transportation," *JoM*, vol. 58, no. 11, pp. 67–70, 2006.
- [19] R. P. M, R. Saravanan, and M. Nagaral, "Fabrication and Wear Behavior of Particulate Reinforced Metal Matrix Composites-An Overview," *IOSR J. Mech. Civ. Eng.*, vol. 14, no. 01, pp. 10–20, 2017.
- [20] K. K. Chawla, "Ceramic matrix composites. (illustrated)." New York: Springer, 2003.
- [21] E. Fitzer, "The future of carbon-carbon composites," *Carbon N. Y.*, vol. 25, no. 2, pp. 163–190, 1987.
- [22] K. S. Shankar, C. Harish, and B. Praharshini, "Fabrication of Fiber Reinforced Composite," pp. 12925–12937, 2016.
- [23] D. D. L. Chung, *Functional Materials: Electrical, Dielectric, Electromagnetic, Optical and Magnetic Applications*, vol. 2. World Scientific Publishing Company, 2010.
- [24] R. Rothon, *Particulate-filled polymer composites*. iSmithers Rapra Publishing, 2003.
- [25] R. H. Krock, *ASTM Proceedings, Vol. 63, 1963. Copyright ASTM, 1916 Race*

- Street, Philadelphia, PA 19103. Reprinted with permission. .*
- [26] P. K. Mallick, “Fiber Reinforced Composites, Materials, Manufacturing, and Design, Marcel Decker,” *Inc., New York*, 1993.
- [27] G. Staab, *Laminar composites*. Butterworth-Heinemann, 1999.
- [28] John Crawford, “[http://plastiquarian.com/?page\\_id=14248](http://plastiquarian.com/?page_id=14248).”
- [29] E. Pawar, “A review article on acrylic PMMA,” *IOSR J. Mech. Civ. Eng. e-ISSN*, vol. 13, no. 2, pp. 1–4, 2016.
- [30] “[https://www.sigmaaldrich.com/catalog/product/aldrich/445746?lang=en&region SX](https://www.sigmaaldrich.com/catalog/product/aldrich/445746?lang=en&region>SX).” .
- [31] R. Q. Frazer, R. T. Byron, P. B. Osborne, and K. P. West, “PMMA: an essential material in medicine and dentistry,” *J. Long. Term. Eff. Med. Implants*, vol. 15, no. 6, 2005.
- [32] R. Bhola, S. M. Bhola, H. Liang, and B. Mishra, “Biocompatible denture polymers-a review,” *Trends Biomater Artif Organs*, vol. 23, no. 3, pp. 129–136, 2010.
- [33] S. E. Park, M. Chao, and P. A. Raj, “Mechanical properties of surface-charged poly (methyl methacrylate) as denture resins,” *Int. J. Dent.*, vol. 2009, 2009.
- [34] U. Ali, K. J. B. A. Karim, and N. A. Buang, “A review of the properties and applications of poly (methyl methacrylate)(PMMA),” *Polym. Rev.*, vol. 55, no. 4, pp. 678–705, 2015.
- [35] G. M. D. Almaraz, A. G. Martínez, R. H. Sánchez, E. C. Gómez, M. G. Tapia, and J. C. V. Juárez, “Ultrasonic Fatigue Testing on the Polymeric Material PMMA, Used in Odontology Applications,” *Procedia Struct. Integr.*, vol. 3, pp. 562–570, 2017.
- [36] J. P. A. Rahamneh, “Oral Dent. 29(2009) 181-183.”
- [37] L. F. R. G. F.C.P.P.D. Souzaa, H. Panzeria, M.A. Vieiraa, “Consanib, Mater Res.12(2009)415-418.”
- [38] M. Stickler , T. Rhein, “Polymethacrylates in Ullmann’s Encyclopedia of Industrial Chemistry, 5th ed., Elvers, B.; Hawkins, S.; Schultz, G. Eds., VHS: New York, 1992, A21, 473. 1992.”

- [39] R. W. Kine, B.B; Novak, "Acrylic and Methacrylic Ester Polymers" in Encyclopedia of Polymer Science and Engineering, Wiley: New York, 1985, 262," 1985.
- [40] H. F. Gruber, "Prog. Polym. Sci.,1992,17,953."
- [41] P. Decker, "Macromol. Symp., 1999, 143,45."
- [42] G. Odian, "Principles of Polymerization, 2nd ed., Wiley: New York, 1981."
- [43] P. Spasojević, V. Panić, S. Šešlija, V. Nikolić, I. G. Popović, and S. Veličković, "Poly (methyl methacrylate) denture base materials modified with ditetrahydrofurfuryl itaconate: Significant applicative properties," *J. Serb. Chem. Soc.*, vol. 80, no. 9, pp. 1177–1192, 2015.
- [44] A. D. Pomogailo, V. N. Kestelman, and G. I. Dzhardimalieva, "Monomeric and polymeric carboxylic acids," in *Macromolecular Metal Carboxylates and Their Nanocomposites*, Springer, 2010, pp. 7–25.
- [45] P. Milson and J. Meers, "Gluconic and itaconic acids, Comprehensive biotechnology. Angewandte Chemie International Edition in English 26: 588.)" Pergamon Press, 1985.
- [46] "[https://pubchem.ncbi.nlm.nih.gov/compound/Itaconic\\_acid](https://pubchem.ncbi.nlm.nih.gov/compound/Itaconic_acid)."
- [47] J. Veličković and S. Vasović, "Kuhn-Mark-Houwink-Sakurada relations and unperturbed dimensions of poly (di-n-alkyl itaconates)," *Die Makromol. Chemie Macromol. Chem. Phys.*, vol. 153, no. 1, pp. 207–218, 1972.
- [48] M. Fernández-Garcia, J. L. De La Fuente, and E. L. Madruga, "Thermal behavior of poly (dimethyl itaconate) and poly (di-n-butyl itaconate) copolymerized with methyl methacrylate," *Polym. Eng. Sci.*, vol. 41, no. 9, pp. 1616–1625, 2001.
- [49] G. J. G. Ruijter, C. P. Kubicek, and J. Visser, "Production of organic acids by fungi," in *Industrial Applications*, Springer, 2002, pp. 213–230.
- [50] M. I. Shtil'man, *Polymeric biomaterials*, vol. 15. VSP, 2003.
- [51] C. Y. K. Lung and B. W. Darvell, "Methyl methacrylate monomer–polymer equilibrium in solid polymer," *Dent. Mater.*, vol. 23, no. 1, pp. 88–94, 2007.
- [52] P. K. Vallittu, V. Miettinen, and P. Alakuijala, "Residual monomer content and its release into water from denture base materials," *Dent. Mater.*, vol. 11, no. 5–6,



- pp. 338–342, 1995.
- [53] S. Y. K. Shirakawa, Y. Adegawa, “(Fuji Photo Film Co., Ltd) US 6,773,862 (2004).”
- [54] K. K. K. Sato, “(Fuji Photo Film Co., Ltd) US 6,777,160 (2004).”
- [55] C. L. A. Berube, “(André Berube) US 6,733,125 (2004).”
- [56] E. R. Lukenbach, C. Kaminski, S. Pascal-Suisse, M. Tahar, and M. Ruggiero, “(Johnson & Johnson Consumer Companies, Inc.) US 6,762,158 (2004).” 2004.
- [57] M. Fernández-García and E. L. Madruga, “Glass transitions in dimethyl and di-n-butyl poly (itaconate ester) s and their copolymers with methyl methacrylate,” *Polymer (Guildf.)*, vol. 38, no. 6, pp. 1367–1371, 1997.
- [58] C. Baudin, “Processing of alumina and corresponding composites”, in *Comprehensive Hard Materials. Ceramics*. L. Ilanes and D. Mari, Eds., Elsevier Ltd., Amsterdam, 2 (2014).”
- [59] M. Kok, “Production and mechanical properties of Al<sub>2</sub>O<sub>3</sub> particle-reinforced 2024 aluminium alloy composites,” *J. Mater. Process. Technol.*, vol. 161, no. 3, pp. 381–387, 2005.
- [60] D. K. Shukla, S. V Kasisomayajula, and V. Parameswaran, “Epoxy composites using functionalized alumina platelets as reinforcements,” *Compos. Sci. Technol.*, vol. 68, no. 14, pp. 3055–3063, 2008.
- [61] P. W. Park, C. S. Ragle, C. L. Boyer, M. Lou Balmer, M. Engelhard, and D. McCready, “In<sub>2</sub>O<sub>3</sub>/Al<sub>2</sub>O<sub>3</sub> catalysts for NO<sub>x</sub> reduction in lean condition,” *J. Catal.*, vol. 210, no. 1, pp. 97–105, 2002.
- [62] A. Drah *et al.*, “Highly ordered macroporous  $\gamma$ -alumina prepared by a modified sol-gel method with a PMMA microsphere template for enhanced Pb<sup>2+</sup>, Ni<sup>2+</sup> and Cd<sup>2+</sup> removal,” *Ceram. Int.*, vol. 43, no. 16, pp. 13817–13827, 2017.
- [63] G. A. Lazouzi *et al.*, “Dimethyl Itaconate Modified PMMA-Alumina Fillers Composites With Improved Mechanical Properties,” *Polym. Compos.*, vol. 40, no. 5, pp. 1691–1701, 2019.
- [64] T. Shirai, H. Watanabe, M. Fuji, and M. Takahashi, “Structural properties and surface characteristics on aluminum oxide powders,” 2010.

- [65] T. Noguchi, K. Matsui, N. M. Islam, Y. Hakuta, and H. Hayashi, "Rapid synthesis of  $\gamma$ -Al<sub>2</sub>O<sub>3</sub> nanoparticles in supercritical water by continuous hydrothermal flow reaction system," *J. Supercrit. Fluids*, vol. 46, no. 2, pp. 129–136, 2008.
- [66] X. Su, S. Chen, and Z. Zhou, "Synthesis and characterization of monodisperse porous  $\alpha$ -Al<sub>2</sub>O<sub>3</sub> nanoparticles," *Appl. Surf. Sci.*, vol. 258, no. 15, pp. 5712–5715, 2012.
- [67] T. Horiuchi, T. Osaki, T. Sugiyama, K. Suzuki, and T. Mori, "Maintenance of large surface area of alumina heated at elevated temperatures above 1300° C by preparing silica-containing pseudoboehmite aerogel," *J. Non. Cryst. Solids*, vol. 291, no. 3, pp. 187–198, 2001.
- [68] J. Li, Y. Pan, C. Xiang, Q. Ge, and J. Guo, "Low temperature synthesis of ultrafine  $\alpha$ -Al<sub>2</sub>O<sub>3</sub> powder by a simple aqueous sol–gel process," *Ceram. Int.*, vol. 32, no. 5, pp. 587–591, 2006.
- [69] M. R. Karim, M. A. Rahman, M. A. J. Miah, H. Ahmad, M. Yanagisawa, and M. Ito, "Synthesis of  $\gamma$ -alumina particles and surface characterization," *Open Colloid Sci. J.*, vol. 4, no. 5, pp. 32–36, 2011.
- [70] K.-L. Huang, L.-G. Yin, S.-Q. Liu, and C.-J. Li, "Preparation and formation mechanism of Al<sub>2</sub>O<sub>3</sub> nanoparticles by reverse microemulsion," *Trans. Nonferrous Met. Soc. China*, vol. 17, no. 3, pp. 633–637, 2007.
- [71] C.-C. Ma, X.-X. Zhou, X. Xu, and T. Zhu, "Synthesis and thermal decomposition of ammonium aluminum carbonate hydroxide (AACH)," *Mater. Chem. Phys.*, vol. 72, no. 3, pp. 374–379, 2001.
- [72] A. I. Y. Tok, F. Y. C. Boey, and X. L. Zhao, "Novel synthesis of Al<sub>2</sub>O<sub>3</sub> nanoparticles by flame spray pyrolysis," *J. Mater. Process. Technol.*, vol. 178, no. 1–3, pp. 270–273, 2006.
- [73] K. Laishram, R. Mann, and N. Malhan, "A novel microwave combustion approach for single step synthesis of  $\alpha$ -Al<sub>2</sub>O<sub>3</sub> nanopowders," *Ceram. Int.*, vol. 38, no. 2, pp. 1703–1706, 2012.
- [74] X. Wang, G. Lu, Y. Guo, Y. Wang, and Y. Guo, "Preparation of high thermal-stabile alumina by reverse microemulsion method," *Mater. Chem. Phys.*, vol. 90,

- no. 2–3, pp. 225–229, 2005.
- [75] M. Boutonnet, J. Kizling, P. Stenius, and G. Maire, “The preparation of monodisperse colloidal metal particles from microemulsions,” *Colloids and surfaces*, vol. 5, no. 3, pp. 209–225, 1982.
- [76] J. Ma and B. Wu, “Effect of surfactants on preparation of nanoscale  $\alpha$ -Al<sub>2</sub>O<sub>3</sub> powders by oil-in-water microemulsion,” *Adv. powder Technol.*, vol. 24, no. 1, pp. 354–358, 2013.
- [77] Z. Zhang and H. Lei, “Preparation of  $\alpha$ -alumina/polymethacrylic acid composite abrasive and its CMP performance on glass substrate,” *Microelectron. Eng.*, vol. 85, no. 4, pp. 714–720, 2008.
- [78] “Alumina (Aluminium Oxide) - The Different Types of Commercially Available Grades”. The A to Z of Materials. 3 May 2002. Archived from the original on 10 October 2007. Retrieved 27 October 2007  
[https://www.azom.com/article.aspx?ArticleID=1389.](https://www.azom.com/article.aspx?ArticleID=1389) .
- [79] L. K. Hudson, C. Misra, A. J. Perrotta, K. Wefers, and F. S. Williams, “Aluminum oxide,” *Ullmann’s Encycl. Ind. Chem.*, 2002.
- [80] “material Properties Data: Alumina (Aluminum Oxide) Archived 2010-04-01 at the Wayback Machine. Makeitfrom.com. Retrieved on 2013-04-17.”
- [81] T. Hooshmand, R. Daw, R. Van Noort, and R. D. Short, “XPS analysis of the surface of leucite-reinforced feldspathic ceramics,” *Dent. Mater.*, vol. 17, no. 1, pp. 1–6, 2001.
- [82] J. G. Marsden, “Organofunctional silane coupling agents,” in *Handbook of adhesives*, Springer, 1990, pp. 536–548.
- [83] J. Jancar and P. Polacek, “Hydrolytically stable interphase on alumina and glass fibers via hydrosilylation,” *Compos. Interfaces*, vol. 18, no. 8, pp. 633–644, 2011.
- [84] “ASTM E384-16 - Stand. Test method microindentation hardness mater. 201528.”
- [85] A. A. Ashor, M. M. Vuksanović, N. Z. Tomić, A. Marinković, and R. Jančić Heinemann, “The influence of alumina particle modification on the adhesion of the polyacrylate matrix composite films and the metal substrate,” *Compos.*

- Interfaces*, vol. 26, no. 5, pp. 417–430, 2019.
- [86] “Standard Method of Vibratory Cavitation Erosion Test (1992) G32-92, Annual Book of ASTM Standards, Vol. 03.02. ASTM, Philadelphia.”
- [87] A. A. Ashor *et al.*, “Optimization of modifier deposition on the alumina surface to enhance mechanical properties and cavitation resistance,” *Polym. Bull.*, pp. 1–18, 2019.
- [88] M. M. Dimitrijević, M. Dojčinović, D. Trifunović, T. Volkov–Husović, and R. J. Hainneman, “Comparison of morphological parameters of ceramic materials surface damage exposed to thermal shock and cavitation erosion,” *Sci. Sinter.*, vol. 48, no. 3, 2016.
- [89] “<https://shop.inkemiagreenchemicals.com/products/used-cooking-oil-fatty-acid-methyl-esters>.” .
- [90] T. Issariyakul and A. K. Dalai, “Biodiesel from vegetable oils,” *Renew. Sustain. Energy Rev.*, vol. 31, pp. 446–471, 2014.
- [91] J. D. Rusmirovic *et al.*, “High performance unsaturated polyester based nanocomposites: Effect of vinyl modified nanosilica on mechanical properties,” *Express Polym. Lett.*, vol. 10, no. 2, pp. 139–159, 2016.
- [92] L. S. Shlyakhtenko, A. A. Gall, and Y. L. Lyubchenko, “Mica functionalization for imaging of DNA and protein-DNA complexes with atomic force microscopy,” in *Cell Imaging Techniques*, Springer, 2012, pp. 295–312.
- [93] “[https://en.wikipedia.org/wiki/\(3-Aminopropyl\)triethoxysilane](https://en.wikipedia.org/wiki/(3-Aminopropyl)triethoxysilane).” .
- [94] L. A. S. A. Prado, M. Sriyai, M. Ghislandi, A. Barros-Timmons, and K. Schulte, “Surface modification of alumina nanoparticles with silane coupling agents,” *J. Braz. Chem. Soc.*, vol. 21, no. 12, pp. 2238–2245, 2010.
- [95] J. Zec, N. Z. Tomić, M. Zrilić, S. Lević, A. Marinković, and R. J. Heinemann, “Optimization of Al<sub>2</sub>O<sub>3</sub> particle modification and UHMWPE fiber oxidation of EVA based hybrid composites: Compatibility, morphological and mechanical properties,” *Compos. Part B Eng.*, vol. 153, pp. 36–48, 2018.
- [96] L. T. Truong *et al.*, “Dispersibility of silane-functionalized alumina nanoparticles in syndiotactic polypropylene,” *Surf. Interface Anal.*, vol. 42, no. 6-7, pp. 1046–

- 1049, 2010.
- [97] S.-Y. Fu, X.-Q. Feng, B. Lauke, and Y.-W. Mai, "Effects of particle size, particle/matrix interface adhesion and particle loading on mechanical properties of particulate-polymer composites," *Compos. Part B Eng.*, vol. 39, no. 6, pp. 933–961, 2008.
- [98] A. A. Algellai *et al.*, "Improvement of cavitation resistance of composite films using functionalized alumina particles.," *Chem. Ind. Ind.*, vol. 72, no. 4, 2018.
- [99] G. Lazouzi *et al.*, "Optimized preparation of alumina based fillers for tuning composite properties," *Ceram. Int.*, vol. 44, no. 7, pp. 7442–7449, 2018.
- [100] J. Zec, N. Tomić, M. Zrilić, S. Marković, D. Stojanović, and R. Jančić-Heinemann, "Processing and characterization of UHMWPE composite fibres with alumina particles in poly (ethylene-vinyl acetate) matrix," *J. Thermoplast. Compos. Mater.*, vol. 31, no. 5, pp. 689–708, 2018.
- [101] D. Chandler, "Interfaces and the driving force of hydrophobic assembly," *Nature*, vol. 437, no. 7059, p. 640, 2005.
- [102] M. A. Ulibarri, M. J. Hernandez, and J. Cornejo, "Hydrotalcite-like compounds obtained by anion exchange reactions," *J. Mater. Sci.*, vol. 26, no. 6, pp. 1512–1516, 1991.
- [103] I. E. Grey and R. Ragozzini, "Formation and characterization of new magnesium aluminum hydroxycarbonates," *J. Solid State Chem.*, vol. 94, no. 2, pp. 244–253, 1991.
- [104] G. Abellán, E. Coronado, C. Martí-Gastaldo, E. Pinilla-Cienfuegos, and A. Ribera, "Hexagonal nanosheets from the exfoliation of Ni<sup>2+</sup>-Fe<sup>3+</sup> LDHs: a route towards layered multifunctional materials," *J. Mater. Chem.*, vol. 20, no. 35, pp. 7451–7455, 2010.
- [105] G. Busca, F. Trifiro, and A. Vaccari, "Characterization and catalytic activity of cobalt-chromium mixed oxides," *Langmuir*, vol. 6, no. 9, pp. 1440–1447, 1990.
- [106] M. Pracella, M. M. Haque, and V. Alvarez, "Compatibilization and Properties of EVA Copolymers Containing Surface-Functionalized Cellulose Microfibers," *Macromol. Mater. Eng.*, vol. 295, no. 10, pp. 949–957, 2010.

- [107] R. McCann, S. S. Roy, P. Papakonstantinou, J. A. McLaughlin, and S. C. Ray, “Spectroscopic analysis of a-C and a-CN x films prepared by ultrafast high repetition rate pulsed laser deposition,” *J. Appl. Phys.*, vol. 97, no. 7, p. 73522, 2005.
- [108] R. V Mladenovic I, Lamovec J, Jovic V, Popovic B, Vorkapic M, “Proceedings of 4th International Conference on Electrical, Electronics and Computing Engineering, IcETRAN 2017 June 05-08, Kladovo, Serbia.”
- [109] A. A. Algellai *et al.*, “The implementation of image analysis for the visualization of adhesion assessment of a composite film,” *Mater. Lett.*, vol. 227, pp. 25–28, 2018.
- [110] T. Kovačević *et al.*, “New composites based on waste PET and non-metallic fraction from waste printed circuit boards: Mechanical and thermal properties,” *Compos. Part B Eng.*, vol. 127, pp. 1–14, 2017.
- [111] M. Chen and J. Gao, “The adhesion of copper films coated on silicon and glass substrates,” *Mod. Phys. Lett. B*, vol. 14, no. 03, pp. 103–108, 2000.
- [112] J. L. He, W. Z. Li, and H. D. Li, “Hardness measurement of thin films: separation from composite hardness,” *Appl. Phys. Lett.*, vol. 69, no. 10, pp. 1402–1404, 1996.
- [113] L. Picard, P. Phalip, E. Fleury, and F. Ganachaud, “Chemical adhesion of silicone elastomers on primed metal surfaces: A comprehensive survey of open and patent literatures,” *Prog. Org. Coatings*, vol. 80, pp. 120–141, 2015.
- [114] S. Ebnesajjad and A. H. Landrock, *Adhesives technology handbook*. UK: Elsevier, 2015.
- [115] A. A. Algellai *et al.*, “Adhesion testing of composites based on Bis-GMA/TEGDMA monomers reinforced with alumina based fillers on brass substrate,” *Compos. Part B Eng.*, vol. 140, pp. 164–173, 2018.
- [116] M. M. Vuksanović *et al.*, “The influence of alumina crystal structures on the morphology and surface erosion of PMMA composite materials exposed to cavitation testing,” *Wear*, vol. 436, p. 203033, 2019.
- [117] P. Elia, E. Nativ-Roth, Y. Zeiri, and Z. Porat, “Determination of the average pore-

- size and total porosity in porous silicon layers by image processing of SEM micrographs,” *Microporous Mesoporous Mater.*, vol. 225, pp. 465–471, 2016.
- [118] M. Dojcinovic and T. Volkov-Husovic, “Cavitation damage of the medium carbon steel: implementation of image analysis,” *Mater. Lett.*, vol. 62, no. 6–7, pp. 953–956, 2008.
- [119] V. Obradović, D. B. Stojanović, I. Živković, V. Radojević, P. S. Uskoković, and R. Aleksić, “Dynamic mechanical and impact properties of composites reinforced with carbon nanotubes,” *Fibers Polym.*, vol. 16, no. 1, pp. 138–145, 2015.
- [120] M. M. Vuksanović, M. Gajić-Kvašček, M. Dojčinović, T. V. Husović, and R. J. Heinemann, “New surface characterization tools for alumina based refractory material exposed to cavitation-Image analysis and pattern recognition approach,” *Mater. Charact.*, vol. 144, pp. 113–119, 2018.

## Изјава о истоветности штампане и електронске верзије докторског рада

Име и презиме аутора Almabrok A. Ashor

Број индекса 4037/2015

Студијски програм Инжењерство материјала

Наслов рада **Uticaj načina ostvarivanja veze između ojačanja i matrice u kompozitu na bazi akrilata i čestica aluminijum-oksida na adheziona i mehanička svojstva kompozita (Influence of interphase bonding in acrylate matrix – alumina reinforcement on mechanical and adhesion properties of composite)**

Ментори др Радмила Јанчић Heinemann редовни професор и др Марија Вуксановић, виши научни сарадник

Изјављујем да је штампана верзија мог докторског рада истоветна електронској верзији коју сам предао/ла ради похрањена у **Дигиталном репозиторијуму Универзитета у Београду**.

Дозвољавам да се објаве моји лични подаци везани за добијање академског назива доктора наука, као што су име и презиме, година и место рођења и датум одбране рада.

Ови лични подаци могу се објавити на мрежним страницама дигиталне библиотеке, у електронском каталогу и у публикацијама Универзитета у Београду.

Потпис аутора

У Београду, 28.01.2020.





## Изјава о коришћењу

Овлашћујем Универзитетску библиотеку „Светозар Марковић“ да у Дигитални репозиторијум Универзитета у Београду унесе моју докторску дисертацију под насловом:

**Uticaj načina ostvarivanja veze između ojačanja i matrice u kompozitu na bazi akrilata i čestica aluminijum-oksida na adheziona i mehanička svojstva kompozita**

**(Influence of interphase bonding in acrylate matrix – alumina reinforcement on mechanical and adhesion properties of composite)**

која је моје ауторско дело.

Дисертацију са свим прилозима предао/ла сам у електронском формату погодном за трајно архивирање.

Моју докторску дисертацију похрањену у Дигиталном репозиторијуму Универзитета у Београду и доступну у отвореном приступу могу да користе сви који поштују одредбе садржане у одабраном типу лиценце Креативне заједнице (Creative Commons) за коју сам се одлучио/ла.

1. Ауторство (CC BY)
2. Ауторство – некомерцијално (CC BY-NC)
3. Ауторство – некомерцијално – без прерада (CC BY-NC-ND)
4. Ауторство – некомерцијално – делити под истим условима (CC BY-NC-SA)
5. Ауторство – без прерада (CC BY-ND)
6. Ауторство – делити под истим условима (CC BY-SA)

(Молимо да заокружите само једну од шест понуђених лиценци.  
Кратак опис лиценци је саставни део ове изјаве).

Потпис аутора

У Београду, 28.01.2020.



#### CV of the candidate

Almabrok A. Ashor was born on 27<sup>th</sup> of February 1965. In Zilten Lybia. He completed education In Lybia in 1989. Compleating the academic studies at the University of Tripoli in the field of materials science and metallurgy. 2010 he completed Master studies in Production engineering. From 1990 to 2002 he worked as engineer in the department of materials properties in Kaam factory. From 2002 to 2010 he was angaged as engineer at Polytechnical institute in Zilten. From 2010 to 2013 he was a lecturer and head of department of mechanical engineering at higher polytechnical institute in Zilten. In 2015 he enroled for the Ph. D. studies at the University of Belgrade. He passed all exams with the average note of 9,93. He has two publications in international journals related to his thesis.

#### Биографија кандидата

Almabrok A. Ashora, дипл. инжењера машинства, рођен је 27. 02. 1965. године у Зилтену у Либији. Школовао се у Либији. 1989, године завршио је основне академске студије на Универзитету у Триполију из области материјала и металургије. 2010. године завршио је мастер студије из Индустријског инжењерства. У периоду од 1990. до 2002. године радио је као инжењер у одељењу за механичка својства материјала за Каам индустрију. Од 2002. до 2010. радио је као инжењер на вишем политехничком институту у Зилтену. Од 2010. до 2013. је предавач и шеф машинског инжењерства на вишем политехничком институту у Зилтену. Године 2015. уписао је докторске студије на Универзитету у Београду и положио све предвиђене испите са средњом оценом 9,93. Има објављена два рада из категорије M22.